AGU PUBLICATIONS

JGR

Journal of Geophysical Research: Atmospheres

RESEARCH ARTICLE

10.1002/2014JD021636

Key Points:

- RCMs do not perform better than GCMs for precipitation extremes
- RCMs and GCMs do not reproduce observed trends in extreme precipitation in India
- RCMs show wet bias in extreme precipitation characteristics over India

Supporting Information:

- Readme
- Figures S1 and S2

Correspondence to:
V. Mishra,
vmishra@iitgn.ac.in

Citation:
Mishra, V., D. Kumar, A. R. Ganguly, J. Sanjay, M. Mujumdar, R. Krishnan, and R. D. Shah (2014), Reliability of regional and global climate models to simulate precipitation extremes over India, *J. Geophys. Res. Atmos.*, *119*, 9301–9323, doi:10.1002/2014JD021636.

Received 13 FEB 2014
Accepted 30 JUN 2014
Accepted article online 2 JUL 2014
Published online 7 AUG 2014

Reliability of regional and global climate models to simulate precipitation extremes over India

Vimal Mishra[1], Devashish Kumar[2], Auroop R. Ganguly[2], J. Sanjay[3], Milind Mujumdar[3], R. Krishnan[3], and Reepal D. Shah[1]

[1]Civil Engineering, Indian Institute of Technology, Gandhinagar, India, [2]Civil and Environmental Engineering, Northeastern University, Boston, Massachusetts, USA, [3]Indian Institute of Tropical Meteorology, Pune, India

Abstract Extreme precipitation events over India have resulted in loss of human lives and damaged infrastructures, food crops, and lifelines. The inability of climate models to credibly project precipitation extremes in India has not been helpful to longer-term hazards resilience policy. However, there have been claims that finer-resolution and regional climate models may improve projections. The claims are examined as hypotheses by comparing models with observations from 1951–2005. This paper evaluates the reliability of the latest generation of general circulation models (GCMs), Coupled Model Intercomparison Project Phase 5 (CMIP5), specifically a subset of the better performing CMIP5 models (called "BEST-GCM"). The relative value of finer-resolution regional climate models (RCMs) is examined by comparing Coordinated Regional Climate Downscaling Experiment (CORDEX) South Asia RCMs ("CORDEX-RCMs") versus the GCMs used by those RCMs to provide boundary conditions, or the host GCMs ("HOST-GCMs"). Ensemble mean of BEST-GCMs performed better for most of the extreme precipitation indices than the CORDEX-RCMs or their HOST-GCMs. Weaker performance shown by ensemble mean of CORDEX-RCMs is largely associated with their high intermodel variation. The CORDEX-RCMs occasionally exhibited slightly superior skills compared to BEST-GCMs; on the whole RCMs failed to significantly outperform GCMs. Observed trends in the extremes were not adequately captured by any of the model ensembles, while neither the GCMs nor the RCMs were determined to be adequate to inform hydrologic design.

1. Introduction

Observations [*Sun et al.*, 2007; *Mishra and Lettenmaier*, 2011; *Mishra et al.*, 2012a, 2012b; *Min et al.*, 2011] and climate models projections [*Kharin et al.*, 2007; *Sillmann et al.*, 2013] suggest increases in precipitation extremes under a warming climate. Increasing trends have been observed over the northern land regions, including the U.S. [*Groisman et al.*, 1999; *Mishra and Lettenmaier*, 2011] and Europe [*Fowler and Ekström*, 2009]. *Coumou and Rahmstorf* [2012] argued that increases in extreme precipitation events under the anthropogenic warming primarily results from the Clausius-Clapeyron relation [*O'Gorman and Schneider*, 2009; *Sugiyama et al.*, 2010; *Mishra et al.*, 2012a, 2012b; *Allan et al.*, 2014], which in turn implies that a warmer atmosphere can hold more water vapor, resulting in heavier precipitation under suitable conditions.

Over the tropics, our understanding of precipitation extremes is less certain [*Kao and Ganguly*, 2011; *Toreti et al.*, 2013]. For instance, over India specifically, studies with observed precipitation extremes have led to disparate conclusions [*Goswami et al.*, 2006; *Ghosh et al.*, 2012; *Vittal et al.*, 2013]. *Goswami et al.* [2006] reported an increasing trend in rainfall extremes over India with a link to climate warming, which was validated and/or refuted in multiple ways by subsequent studies [*Rajeevan et al.*, 2008; *Ghosh et al.*, 2012; *Krishnamurthy et al.*, 2009; *Mani et al.*, 2009; *Kishtawal et al.*, 2010]. For instance, *Ghosh et al.* [2012] reported a lack of uniform trends in extreme precipitation over India but found an increasing trend in the spatial variability of these extremes. An analysis of Coupled Model Intercomparison Project Phase 5 (CMIP5) simulations reported a consistent positive trend in frequency of extreme precipitation days (e.g., > 40 mm/day) for decades beyond 2060 [*Chaturvedi et al.*, 2012].

An increased frequency and intensity of extreme precipitation events may cause flooding and flash floods [*Christensen and Christensen*, 2003; *Fowler and Wilby*, 2010; *Rosenberg et al.*, 2010], which are among the most frequent natural disasters in India [*Mohapatra and Singh*, 2003]. In India, floods affected about 33 million people between 1953 and 2000. Moreover, flood risks in India have substantially increased during the last few decades [*Guhathakurta et al.*, 2011]. During recent years, extreme precipitation events resulted in several damaging floods (e.g., Mumbai in July 2005; Chennai in October and December 2005; Bangalore in October 2005) including the most recent in Uttarakhand in June 2013 which has resulted in a loss of about 6000 human lives (according to the government of Uttarakhand).

Considering the implications of precipitation extremes, several studies focused on understanding the nature and magnitude of extreme precipitation events in the general circulation models (GCMs) [*Kharin and Zwiers*, 2000; *Kharin et al.*, 2007; *Min et al.*, 2011]. However, the ability of the GCMs to adequately reproduce the intensity, duration, and frequency of observed precipitation extremes is a major challenge, and the simulated estimates of extreme precipitation have large uncertainties particularly in the subtropics and tropics [*Toreti et al.*, 2013]. Deficiency in extreme precipitation simulation may be partly due to the coarse resolution in GCMs [*Salathe et al.*, 2010; *Wehner et al.*, 2010]. On the other hand, it is believed that estimates of extreme precipitation events from regional climate models (RCMs) may be more reliable due to better representation of smaller-scale topographic features and physical processes [*Gutowski et al.*, 2010; *Leung et al.*, 2004]. However, *Rummukainen et al.* [2001] and *Déqué et al.* [2007] argued that using RCM data may lead to increased uncertainty due to spatial resolution, numerical scheme, boundary condition, and physical parameterization. *Gutowski et al.* [2003] reported that a high resolution is required to improve intensity of precipitation at shorter durations. However, *Kawazoe and Gutowski* [2013] argued that among the CMIP5 GCMs, the coarsest models generally produce similar precipitation extremes to those of the finest resolution models, which indicates that high resolution may not necessarily improve precipitation extremes. Furthermore, they found that extreme precipitation events in RCMs are more representative than those in GCMs. *Fowler et al.* [2007a, 2007b] found that spatial resolution and number of GCMs used for boundary conditions in RCMs should be considered for designing future ensemble experiments.

It is not yet clear if dynamically downscaled precipitation obtained from the regional climate models provides better skills than GCMs in simulating extreme precipitation events [*Racherla et al.*, 2012; *Laprise*, 2014]. In particular, a rigorous assessment of GCMs and RCMs in simulating the observed characteristics of daily precipitation extremes over the Indian region has been lacking. Here we evaluate the performance of the CMIP5 GCMs and RCMs from the Coordinated Regional Climate Downscaling Experiment (CORDEX) South Asia and their host GCMs against observed precipitation extremes in India. The overarching science question we intend to address is *to what extent can regional climate models provide better information for precipitation extremes as compared to CMIP5 GCMs*? We evaluate GCMs and RCMs for the multiple extreme precipitation indices as well as their large-scale and convective characteristics for the historic period (1951–2005).

2. Methods

Observed daily precipitation data were obtained from the Asian Precipitation-Highly Resolved Observational Data Integration Towards Evaluation (APHRODITE) of water Resource [*Yatagai et al.*, 2012] over 1951–2005 at 0.5° spatial resolution. The data set was generated using the 2500 observation stations located across India. The APHRODITE data set is quality controlled well and thoroughly checked for errors and inconsistencies. Heavy rainfall in the Western Ghats and Himalayan regions is well captured in the APHRODITE data [*Yatagai et al.*, 2012], and the data set better resolves orographic precipitation in the Western Ghats and foothills of the Himalaya. Daily precipitation from the *historical* runs for the period of 1951–2005 was obtained from 32 CMIP5 [*Taylor et al.*, 2012] models at available spatial resolutions (Table 1). We obtained daily precipitation data at 0.5° spatial resolution for the period of 1951–2005 from the four RCMs that participated in the Coordinated Regional Climate Downscaling Experiment (CORDEX) South Asia: COSMO-CLM, RegCM4-GFDL, RegCM4-LMDZ, and SMHI-RCA4. The CORDEX South Asia data set can be obtained from the Center for Climate Change Research website http://cccr.tropmet.res.in/cordex/files/downloads.jsp. Daily precipitation data for the same period were also obtained from the host GCMs (MPI-ESM-LR, GFDL-ESM2M, IPSL-CM5A-LR, and EC-EARTH, Table 1) that were used in the CORDEX downscaling experiment.

Out of the 32 CMIP5 GCMs, we selected the four GCMs (CMCC-CMS, CNRM-CM5, GFDL-CM3, and MPI-ESM-MR, Table 3) that showed a better performance for precipitation extremes during the historic period (1961–1990) over India. To select the BEST-GCMs, we first interpolated daily precipitation from all the selected models at the spatial resolution (0.5°) of the CORDEX-RCMs. Based on all-India median bias in annual maximum precipitation (AMP) during the period of 1961–1990, the four best models were selected. However, interpolation of daily precipitation to higher than the inherent resolution of the models may lead to changes in precipitation intensity and therefore can affect model performance assessed at different spatial resolution [*Chen and Knutson*, 2008;

Table 1. Details of the CMIP5 Models That Were Used for the Analysis

Modeling Center (or Group)	Model Name	Grid Size
Commonwealth Scientific and Industrial Research Organization (CSIRO) and Bureau of Meteorology (BOM), Australia	ACCESS1.0	192 × 145
	ACCESS1.3	192 × 145
Beijing Climate Center, China Meteorological Administration	BCC-CSM1.1	128 × 64
College of Global Change and Earth System Science, Beijing Normal University	BNU-ESM	128 × 64
Canadian Centre for Climate Modelling and Analysis	CanCM4	128 × 64
	CanESM2	128 × 64
National Center for Atmospheric Research	CCSM4	188 × 192
Centro Euro-Mediterraneo per I Cambiamenti Climatici	CMCC-CESM	96 × 48
	CMCC-CM	480 × 240
	CMCC-CMS	192 × 96
Centre National de Recherches Météorologiques/Centre Européen de Recherche et Formation Avancée en Calcul Scientifique	CNRM-CM5	256 × 128
Commonwealth Scientific and Industrial Research Organization in Collaboration with Queensland Climate Change Centre of Excellence	CSIRO-Mk3.6.0	192 × 96
EC-EARTH consortium	EC-EARTH	320 × 160
NOAA Geophysical Fluid Dynamics Laboratory	GFDL-CM3	144 × 90
	GFDL-ESM2G	144 × 90
	GFDL-ESM2M	144 × 90
Met Office Hadley Centre (additional HadGEM2-ES realizations contributed by Instituto Nacional de Pesquisas Espaciais)	HadCM3	96 × 73
	HadGEM2-CC	192 × 145
	HadGEM2-ES	192 × 145
Institute for Numerical Mathematics	INM-CM4	180 × 120
Institut Pierre-Simon Laplace	IPSL-CM5A-LR	96 × 96
	IPSL-CM5A-MR	144 × 143
	IPSL-CM5B-LR	96 × 96
Japan Agency for Marine-Earth Science and Technology, Atmosphere and Ocean Research Institute (The University of Tokyo), and National Institute for Environmental Studies	MIROC-ESM	128 × 64
	MIROC-ESM-CHEM	128 × 64
Atmosphere and Ocean Research Institute (The University of Tokyo), National Institute for Environmental Studies, and Japan Agency for Marine-Earth Science and Technology	MIROC4h	640 × 320
	MIROC5	256 × 128
Max-Planck-Institut für Meteorologie (Max Planck Institute for Meteorology)	MPI-ESM-LR	192 × 96
	MPI-ESM-MR	192 × 96
	MPI-ESM-P	192 × 96
Meteorological Research Institute	MRI-CGCM3	320 × 160
Norwegian Climate Centre	NorESM1-M	144 × 96

Harding et al., 2013]. To test the influence of interpolation on bias in AMP, we interpolated daily precipitation from the CMIP5 models at 0.5 and 1.0° spatial resolutions (Table 3 and Figure 1). We found that the spatial structure of bias in AMP remains almost the same over India for the two resolutions (Figures 1a and 1c); however, all-India median bias for the individual models varies with the resolution (Figures 1b and 1d). For instance, at 0.5° spatial resolution the four best models were CMCC-CMS, CNRM-CM5, GFDL-CM3, and MPI-ESM-MR, while at 1° spatial resolution the four best models were CCSM4, CNRM-CM5, CMCC-CM, and MIROC5 (Table 1 and Figure 1). These differences in bias at the two spatial resolutions can be attributed to the changes in precipitation intensity at 0.5 and 1.0°. Since precipitation from the CORDEX-RCMs is at 0.5° resolution, we selected the four CMIP5 models that performed better at 0.5°. We interpolated CMIP5 models to check how they perform against the CORDEX-RCMs rather than evaluate them against observations as reported in *Racherla et al.* [2012]. Moreover, one may notice that the "BEST-GCMs" are different than the "HOST-GCMs" as they were solely selected based on their performance to simulate extreme precipitation over India. On the other hand, the selection of the HOST-GCMs for boundary conditions of the CORDEX-RCMs could be associated with their overall ability to simulate the Indian Monsoon and the large-scale atmospheric variables. In selecting the HOST-GCMs, it was ensured that the large-scale features of the South Asian monsoon are well captured; however, they were not specifically evaluated for their performance in simulating extreme precipitation events

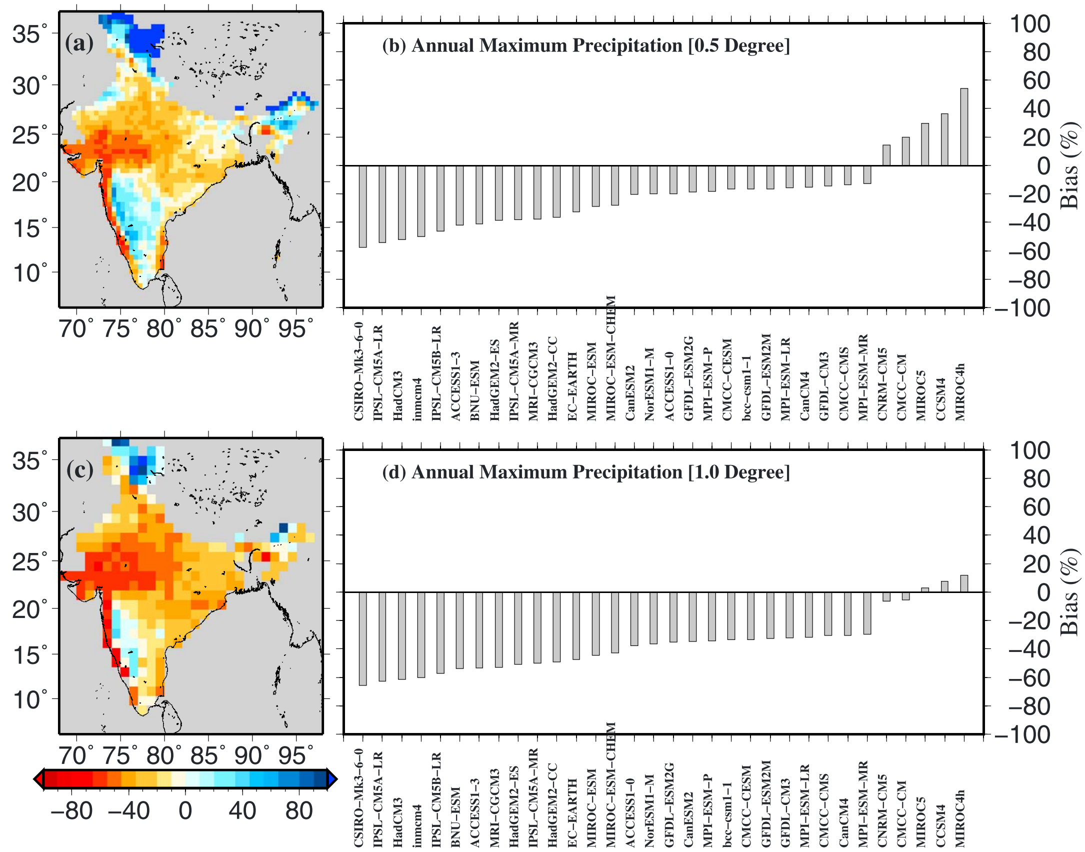

Figure 1. (a) Multimodel ensemble mean bias in annual maximum precipitation at 0.5° spatial resolution, (b) all-India median bias in annual maximum precipitation for the individual CMIP5 models, (c) same as Figure 1a but for the 1° spatial resolution, and (d) same as Figure 1b but for 1° spatial resolution. Bias was estimated against APHRODITE data for the period of 1961–1990.

in the Indian monsoon region. However, *Menon et al.* [2013] reported that IPSL-CM5A-LR, which is one of the HOST-GCMs (Table 2), poorly simulates the Indian monsoon.

Daily precipitation data from the CMIP5 GCMs were interpolated to common grid mesh (0.5°) of the CORDEX-RCMs and APHRODITE to evaluate skills of GCMs and RCMs in simulating extreme precipitation events over India. A bilinear interpolation was performed using the Climate Data Operator (CDO). We tested various methods available for interpolation in CDO and found minimal differences in interpolated daily precipitation intensities. However, we did not use a more sophisticated method such as kriging, which may be considered in future work. We obtained daily surface wind data at 10 m (horizontal component u and vertical component v) from the National Centers for Environmental Prediction/National Center for Atmospheric Research (NCEP-NCAR) reanalysis [*Kalnay et al.*, 1996] to evaluate wind fields from the RCMs and GCMs during the extreme precipitation events. At the selected locations in India, composites of wind fields for the 20 largest extreme precipitation events during 1951–2005 were constructed using the data from the RCMs/GCMs, which were compared against the observed composites based on the NCEP-NCAR reanalysis data sets. To do

Table 2. Regional Climate Models That Participated in the CORDEX South Asia and Their Host GCMs

CORDEX-RCM (Spatial Resolution 0.5°)	HOST-GCM	Spatial Resolution (HOST-GCMs)
COSMO-CLM[a]	MPI-ESM-LR	1.875 × 1.865°
RegCM4-GFDL[b]	GFDL-ESM2M	2.5 × 2.0°
RegCM4-LMDZ[c]	IPSL-CM5A-LR	1.875 × 3.75°
SMHI-RCA4[d]	EC-EARTH	1.125 × 1.125°

[a]Consortium for Small-scale Modeling - Climate Limited-area Modeling community.
[b]Regional Climate Model- Geophysical Fluid Dynamics Laboratory.
[c]Regional Climate Model- Laboratoire de Météorologie Dynamique Zoom.
[d]Swedish Meteorological and Hydrological Institute - Rossby Centre regional Atmospheric model, v4.

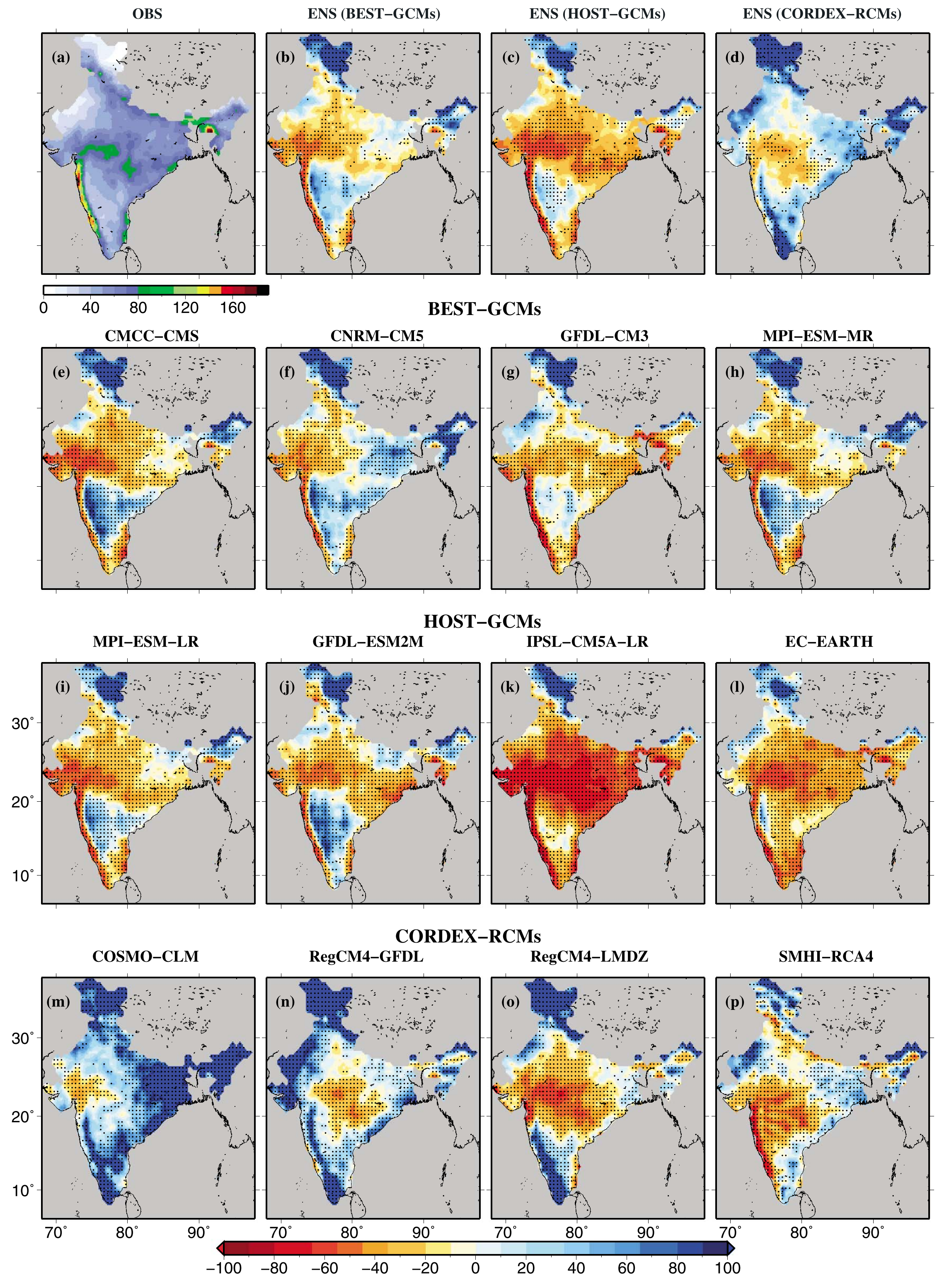

Figure 2. (a) Observed mean annual maximum precipitation (AMP) for the period of 1951–2005; (b–d) ensemble mean bias (%) in AMP in the BEST-GCMs (CMCC-CMS, CNRM-CM5, GFDL-CM3, and MPI-ESM-MR), HOST-GCMs (MPI-ESM-LR, GFDL-ESM2M, IPSL-CM5A-LR, and EC-EARTH), and CORDEX-RCMs (COSMO-CLM, RegCM4-GFDL, RegCM4-LMDZ, and SMHI-RCA4); and (e–p) bias for the individual models in the BEST-GCMs, HOST-GCMs, and CORDEX-RCMs. Bias (%) for the BEST-GCMs, HOST-GCMs, and CORDEX-RCMs was estimated for the period of 1951–2005. Stippling shows grid cells where mean is significantly different than observed mean as estimated by the rank sum test. Stippling in Figures 2b–2d shows grid cells where mean is significantly different than observed mean in all the models in the BEST-GCMs, HOST-GCM, and CORDEX-RCMs.

this, we first selected the top 20 extreme precipitation events based on their magnitude over the three selected locations: Mumbai, Delhi, and Dehradun. For each of the selected extreme precipitation events, we obtained daily wind data. Finally, for all the 20 events, we constructed composites (by taking mean of the selected events) for wind fields.

Annual maximum precipitation, average number of rainy days (precipitation > 1 mm/d), frequency of precipitation extremes (P-FREQ), mean precipitation intensity of the top five events (PI-5), and heavy-to-nonheavy precipitation ratio (H-NH) based on the 99th percentile of rainy days were calculated. Annual maximum precipitation and PI-5 were estimated for each year by obtaining the single largest precipitation event and mean intensity of the top five precipitation events, respectively, during the period of 1951–2005 from the observed and the model-simulated data sets. On the other hand, P-FREQ and H-NH were estimated based on the 99th percentile value of rainy days during the reference period (1961–1990). For each year, P-FREQ was estimated as the number of precipitation events exceeding the 99th percentile of precipitation during the period of 1961–1990. We estimated H-NH by obtaining total precipitation caused by extreme precipitation events ($P >$ 99th percentile of rainy days in 1961–1990) in each year and then dividing by total precipitation due to nonheavy precipitation events. The number of rainy days was estimated to understand relationship between frequency and magnitude of precipitation in the observed and model-simulated data sets. Annual precipitation maxima at the selected durations (1–10 day) and return periods (25–100 years) were estimated using the generalized extreme value (GEV) distribution. The GEV distribution is a three-parameter distribution which represents location, shape, and scale of extremes in the data set. The GEV distribution has been widely used to analyze climate extremes [*Fowler et al.*, 2007a, 2007b; *Kao and Ganguly*, 2011; *Mishra et al.*, 2012a, 2012b]. We estimated the parameters of the GEV distributions for each grid cell over India using the method based on L moments [*Hosking and Wallis*, 2005; *Rosenberg et al.*, 2010; *Mishra et al.*, 2012a, 2012b]. The approach based on L moments is less biased toward outliers present in the data set.

We estimated changes in annual maximum precipitation using the nonparametric Mann-Kendall [*Mann*, 1945] test and Sen's slope method [*Sen*, 1968]. The influence of spatial and temporal correlations on trends in precipitation extremes was taken care of using the method described in *Yue and Wang* [2002]. The Mann-Kendall trend test has been widely used to estimate trends in hydrologic and climatic time series [*Mishra et al.*, 2010; *Mishra and Lettenmaier*, 2011]. To test if precipitation extremes in the models are significantly different than that in observations, the two-sided rank sum test was used to test the statistical significance. For each grid cell, the two-sided rank sum test was applied at 5% level to identify the geographical locations with disagreements between the observed and the model-simulated extreme precipitation characteristics. Bias in extreme precipitation indices was estimated using annual mean observed and model-simulated index for the period of 1951–2005. To estimate ensemble mean bias, we first estimated bias in extreme precipitation indices from the individual models and then mean bias for all the four models was taken.

3. Results and Discussion

3.1. Bias in Extreme Precipitation Characteristics

Figure 2 shows observed annual maximum precipitation (AMP) and bias (%) in the BEST-GCMs, HOST-GCMs, CORDEX-RCMs, and their ensemble mean (ENS) for the period of 1951–2005. Observed AMP varied between 20 and 200 mm with higher values in the Western Ghats and Northeast India and with lower amounts in the semiarid region of western India (Figure 2a). A majority of the CMIP5 models among the BEST-GCMs underestimated observed AMP in central and western India (Figures 2e–2h). On the other hand, most of the BEST-GCMs and their ensemble mean showed a positive bias in peninsular India, Jammu and Kashmir, and northeastern India (Figures 2b and 2e–2h), while bias was negative in the Western Ghats region (Figure 2b). On the other hand, a majority of the HOST-GCMs (Figures 2i–2l) and their ensemble mean (Figure 2c) underestimated mean AMP across India except the northern and northeastern parts. Similarly, most of the CORDEX-RCMs and their ensemble mean overestimated mean AMP in the northern and northeastern region (Figures 2d and 2m–2p), while their ensemble mean underestimated mean AMP in the central parts of India (Figure 2p). All-India median percentage bias in mean AMP varied between −16 and 9, −53 and −14, and −4 and 54% in the BEST-GCMs, HOST-GCMs, and CORDEX-RCMs, respectively (Table 4). Furthermore, ensemble mean bias in AMP in the BEST-GCMs, HOST-GCMs, and CORDEX-RCMs was −6.5, −27, and 21%, respectively (Table 4). The BEST-GCMs showed better performance than that of the CORDEX-RCMs and their HOST-GCMs (Table 4).

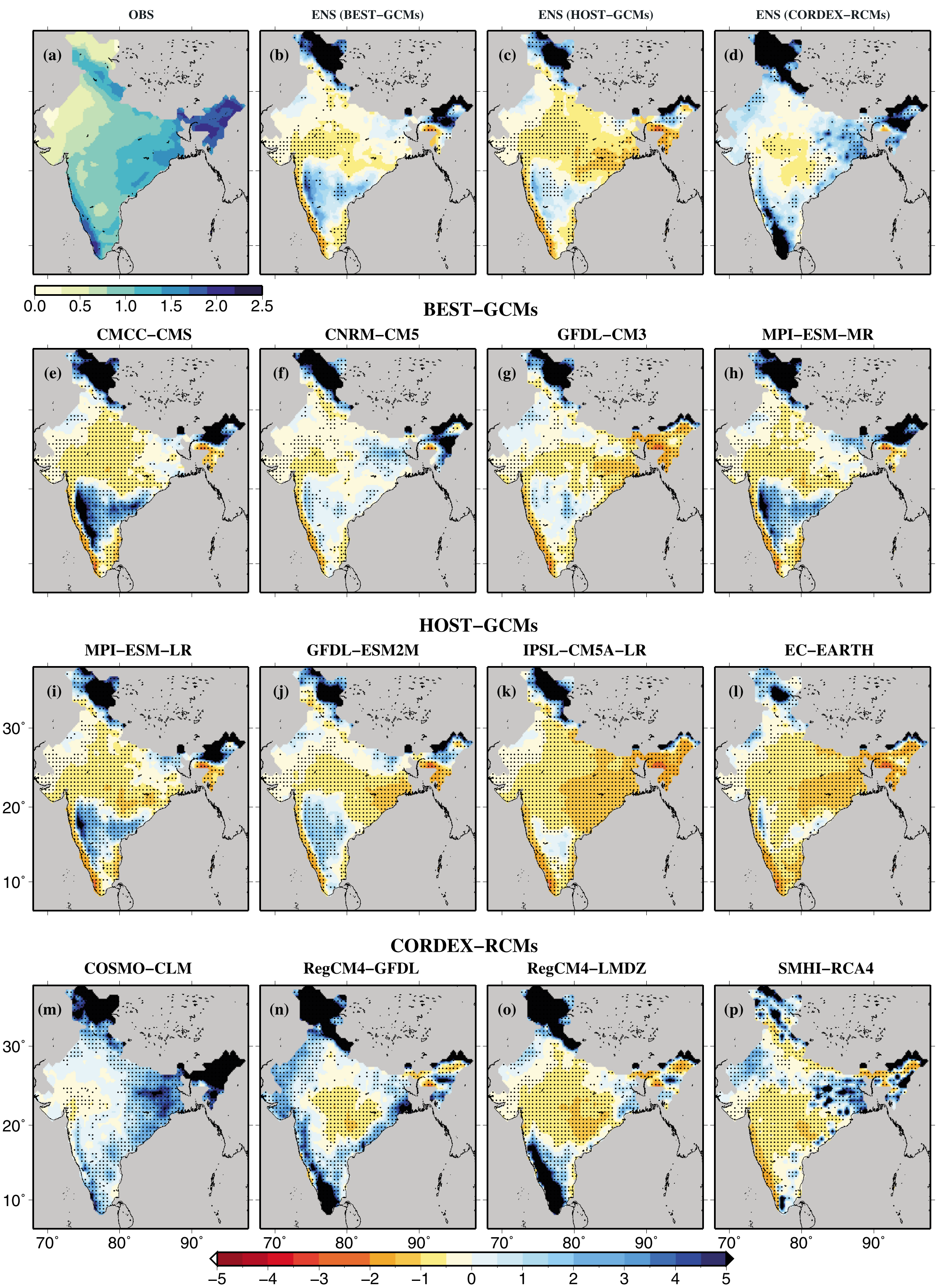

Figure 3. (a) Observed mean frequency of extreme precipitation events (P-FREQ) for the period of 1951–2005; (b–d) ensemble mean bias (events/year) in P-FREQ in the BEST-GCMs (CMCC-CMS, CNRM-CM5, GFDL-CM3, and MPI-ESM-MR), HOST-GCMs (MPI-ESM-LR, GFDL-ESM2M, IPSL-CM5A-LR, and EC-EARTH), and CORDEX-RCMs (COSMO-CLM, RegCM4-GFDL, RegCM4-LMDZ, and SMHI-RCA4); and (e–p) bias for the individual models in the BEST-GCMs, HOST-GCMs, and CORDEX-RCMs. Bias for the BEST-GCMs, HOST-GCMs, and CORDEX-RCMs was estimated for the period of 1951–2005. Stippling shows grid cells where mean is significantly different than observed mean as estimated by the rank sum test. Stippling in Figures 3b–3d shows grid cells where mean is significantly different than observed mean in all the models in the BEST-GCMs, HOST-GCM, and CORDEX-RCMs.

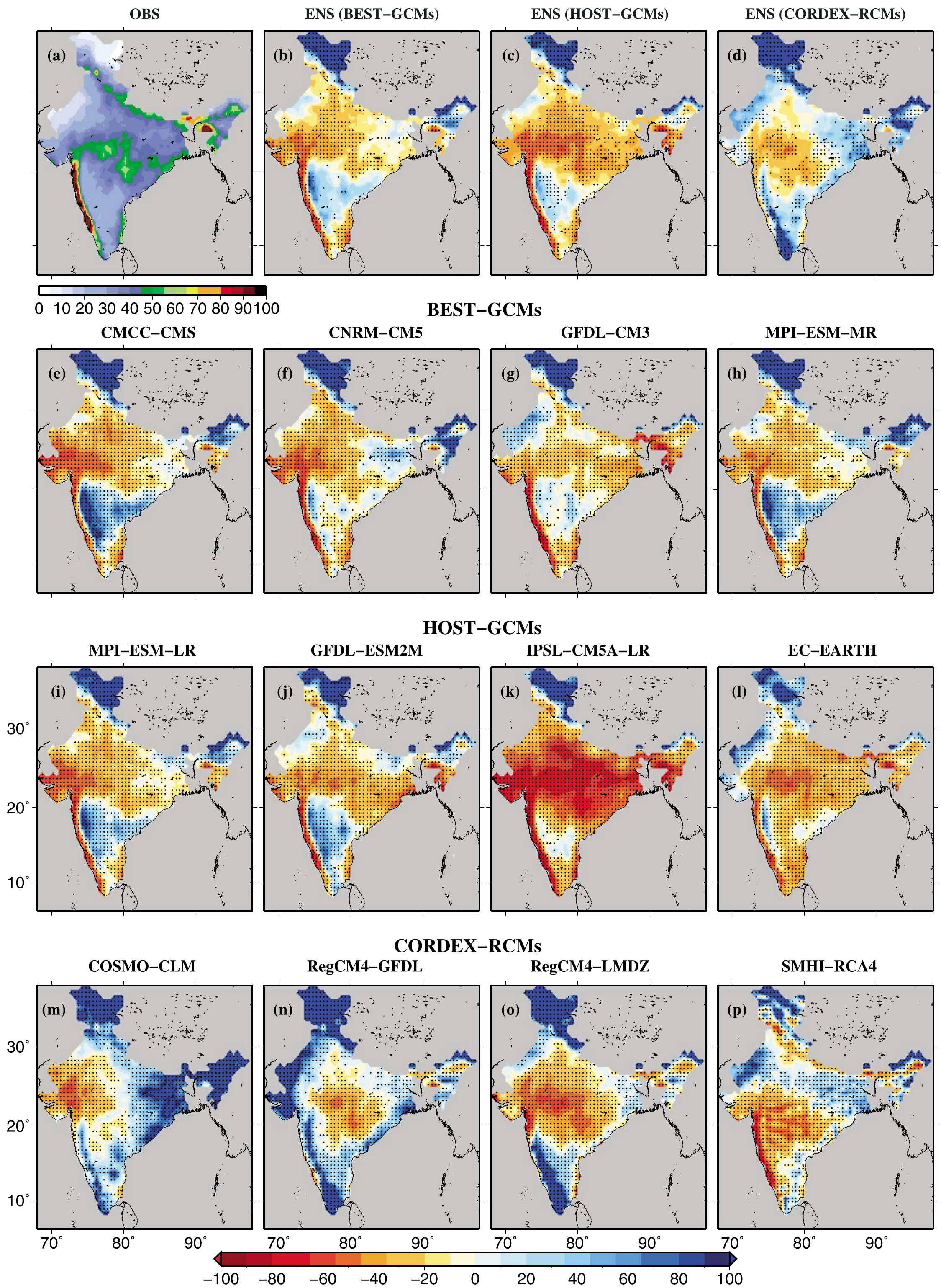

Figure 4. (a) Observed mean intensity (mm) of the top five extreme precipitation events in each year (PI-5) for the period of 1951–2005; (b–d) ensemble mean bias (%) in PI-5 in the BEST-GCMs (CMCC-CMS, CNRM-CM5, GFDL-CM3, and MPI-ESM-MR), HOST-GCMs (MPI-ESM-LR, GFDL-ESM2M, IPSL-CM5A-LR, and EC-EARTH), and CORDEX-RCMs (COSMO-CLM, RegCM4-GFDL, RegCM4-LMDZ, and SMHI-RCA4); and (e–p) bias for the individual models in the BEST-GCMs, HOST-GCMs, and CORDEX-RCMs. Bias for the BEST-GCMs, HOST-GCMs, and CORDEX-RCMs was estimated for the period of 1951–2005. Stippling shows grid cells where mean is significantly different than observed mean as estimated by the rank sum test. Stippling in Figures 4b–4d shows grid cells where mean is significantly different than observed mean in all the models in the BEST-GCMs, HOST-GCM, and CORDEX-RCMs.

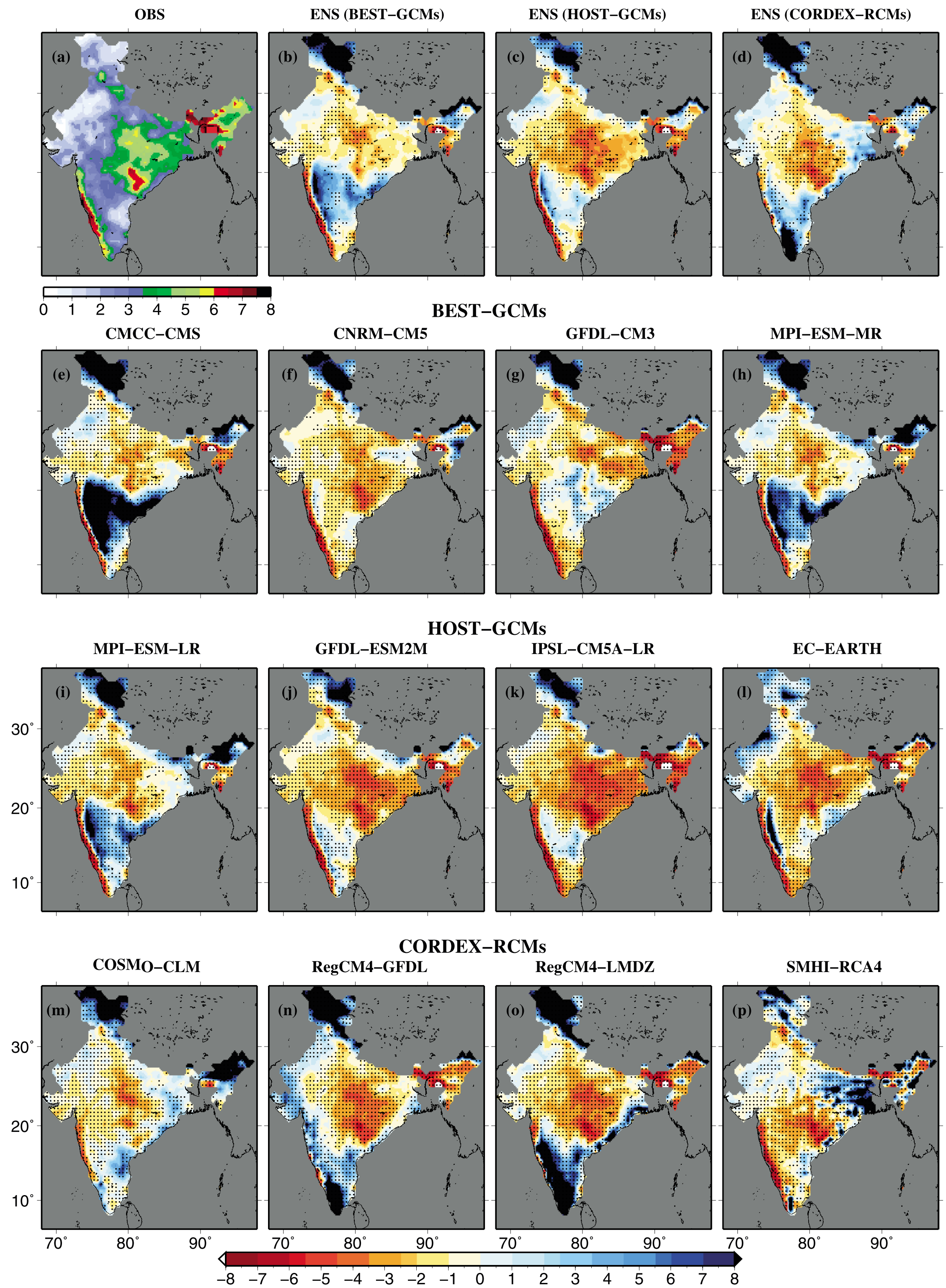

Figure 5. (a) Observed (%) mean heavy-to-nonheavy ratio (H-NH) for each year for the period of 1951–2005; (b–d) ensemble mean bias (%) in H-NH in the BEST-GCMs (CMCC-CMS, CNRM-CM5, GFDL-CM3, and MPI-ESM-MR), HOST-GCMs (MPI-ESM-LR, GFDL-ESM2M, IPSL-CM5A-LR, and EC-EARTH), and CORDEX-RCMs (COSMO-CLM, RegCM4-GFDL, RegCM4-LMDZ, and SMHI-RCA4); and (e–p) bias for the individual models in the BEST-GCMs, HOST-GCMs, and CORDEX-RCMs. Bias for the BEST-GCMs, HOST-GCMs, and CORDEX-RCMs was estimated for the period of 1951–2005. Stippling shows grid cells where mean is significantly different than observed mean as estimated by the rank sum test. Stippling in Figures 5b–5d shows grid cells where mean is significantly different than observed mean in all the models in the BEST-GCMs, HOST-GCM, and CORDEX-RCMs.

Observed mean frequency of extreme precipitation events (P-FREQ) and bias in the BEST-GCMs, HOST-GCMs, and CORDEX-RCMs are shown in Figure 3. Observed mean P-FREQ varied between 0.5 and 2.5 events per year during the period of 1951–2005 with higher frequency in the Western Ghats and Northeast India and lesser events in the semiarid Western India (Figure 3a). Similar to mean AMP, P-FREQ was overestimated in the northern, peninsular, and northeastern India by a majority of the models in the BEST-GCMs, HOST-GCMs, and CORDEX-RCMs. On the other hand, a majority of the CORDEX-RCMs and their HOST-GCMs underestimated P-FREQ in central India (Figure 3). All-India median bias in P-FREQ varied between −0.04 and 0.30, −0.27 and −0.82, and −0.29 and 0.82 events per year in the BEST-GCMs, HOST-GCMs, and CORDEX-RCMs, respectively (Table 4). Ensemble mean biases in P-FREQ for the BEST-GCMs, HOST-GCMs, and CORDEX-RCMs were 0.16, −0.49, and 0.49 events per year, respectively (Table 4), which highlight that the BEST-GCMs perform better than the CORDEX-RCMs to simulate frequency of extreme precipitation events in India.

Figure 4 shows observed mean precipitation intensity for the top five events in each year (PI-5) during the period of 1951–2005 and percentage bias in the BEST-GCMs, HOST-GCMs, and CORDEX-RCMs. Observed mean PI-5 varied between 5 and 100 mm with lower values in the semiarid western India and larger PI-5 in the Western Ghats and Northeast India (Figure 4a). Similar to AMP and P-FREQ, a majority of the RCMs and GCMs overestimated PI-5 in the northern, peninsular, and Northeast India (Figure 4). On the other hand, most of the models and their ensemble mean underestimated PI-5 in central India (Figures 4e–4p). The negative bias present in the HOST-GCMs was somewhat improved in the CORDEX-RCMs; however, the CORDEX-RCMs showed a higher positive bias in many regions (Figures 4m–4o). All-India median bias in PI-5 varied between −9 and 14.5, −13 and 50, and −5 to 24% in the BEST-GCMs, HOST-GCMs, and CORDEX-RCMs, respectively (Table 4). Ensemble mean bias in PI-5 was −10.6, −24, and 11% in the BEST-GCMs, HOST-GCMs, and CORDEX-RCMs, respectively (Table 4).

We estimated the ratio of heavy-to-nonheavy precipitation totals (H-NH) for each year and bias in the GCMs and RCMs for the period of 1951–2005 (Figure 5). Heavy-to-nonheavy ratio varied between 0.5 and 8% with higher values in the Western Ghats, east central region, and northeastern India, while similar to the other indices, lower values were centered in the semiarid western India (Figure 5a). Most of the models overestimated H-NH in the northern, northeastern, and peninsular India and underestimated H-NH in the central India and Western Ghats (Figure 5). Among the BEST-GCMs, GFDL-CM3 and CNRM-CM5 underestimated H-NH in central India (Figures 5f and 5g), while CMCC-CMS and MPI-ESM-MR overestimated H-NH in peninsular India (Figures 5e and 5h). Most of the CORDEX-RCMs and their ensemble mean underestimated H-NH in central India but with a lower bias than that of the HOST-GCMs (Figures 5m–55p). All-India median bias varied between −0.05 and −1.2, −0.4 and −2, and −0.16 and −0.95% among the BEST-GCMs, HOST-GCMs, and CORDEX-RCMs, respectively (Table 4). Moreover, ensemble mean bias showed that the BEST-GCMs outperformed the HOST-GCMs and CORDEX-RCMs with −0.53, −1.3, and 0.97% bias, respectively (Table 4).

We notice that the performance to simulate extreme precipitation was slightly improved in the CORDEX-RCMs in comparison to their HOST-GCMs. However, the BEST-GCMs outperformed both the CORDEX-RCMs as well as their HOST-GCMs for most of the selected extreme precipitation indices. Intermodel variations in the CORDEX-RCMs was higher than that of the BEST-GCMs, whereas for most of the extreme precipitation indices COSMO-CLM and RegCM4-LMDZ showed high positive and negative biases, respectively. These differences in intermodal variations may be related to the numerical scheme, physical parameterization, and boundary conditions used in the regional climate models [*Rummukainen et al.*, 2001]. A high intermodel variation in the CORDEX-RCMs may lead to a high uncertainty in extreme precipitation projections. We further notice that the improvement in the CORDEX-RCMs is not substantial to simulate AMP and PI-5 (see ensemble mean bias for comparison). For instance, overestimations (underestimations) in the northern (central) regions remained somewhat unchanged in the CORDEX-RCMs. However, in the Western Ghat region, the CORDEX-RCMs showed a better performance than the CMIP5 models, which could be attributed to their ability to resolve topography and orographic precipitation. While most of the CMIP5 models in Table 3 displayed dry bias, which is consistent with the findings of *Kawazoe and Gutowski* [2013] and, the BEST-GCMs (CMCC-CMS, CNRM-CM5, GFDL-CM3, and MPI-ESM-MR) showed a better performance to simulate extreme precipitation over India (Table 3). Moreover, we do not notice any direct relationship between the CMIP5 model resolution (Table 1) and the bias in simulating extreme precipitation. However, an improved parameterization related to convection and aerosol schemes in the GCMs plays a major role in better simulation of orographic precipitation and precipitation extremes (see *Watanabe et al.* [2010] for details).

Table 3. All-India Median Bias (%) in Annual Maximum Precipitation (AMP) at 0.5 and 1.0° Spatial Resolutions

CMIP5 Model	Bias AMP (0.5°, %)	Bias AMP (1°, %)
ACCESS1-0	−19.88	−37.8
ACCESS1-3	−41.89	−53.36
BNU-ESM	−41.36	−53.91
CCSM4	36.38	7.49
CMCC-CESM	−16.79	−33.36
CMCC-CM	19.61	−5.53
CMCC-CMS	−13.43	−30.75
CNRM-CM5	14.25	−6.52
CSIRO-Mk3-6-0	−57.54	−65.71
CanCM4	−15.29	−30.48
CanESM2	−20.3	−35
EC-EARTH	−32.8	−47.38
GFDL-CM3	−14.63	−32.21
GFDL-ESM2G	−18.56	−35.38
GFDL-ESM2M	−16.6	−32.75
HadCM3	−51.95	−61.44
HadGEM2-CC	−36.4	−49.38
HadGEM2-ES	−38.59	−50.73
IPSL-CM5A-LR	−54.08	−62.88
IPSL-CM5A-MR	−38.21	−49.93
IPSL-CM5B-LR	−46.38	−57.18
MIROC-ESM	−28.86	−44.63
MIROC-ESM-CHEM	−28.15	−42.8
MIROC4h	54.06	11.55
MIROC5	29.5	2.7
MPI-ESM-LR	−15.65	−31.88
MPI-ESM-MR	−12.76	−29.94
MPI-ESM-P	−18.16	−34.21
MRI-CGCM3	−37.97	−52.86
NorESM1-M	−20.12	−36.68
bcc-csm1-1	−16.78	−33.67
inmcm4	−50.17	−60.03

3.2. Bias in Number of Rainy Days

We evaluated bias in number of rainy days in the selected models to understand if there is any relationship between models' ability to simulate number of rainy days and extreme precipitation indices. Figure 6 shows observed mean annual number of rainy days (precipitation $>$ 1 mm) and bias in the BEST-GCMs, HOST-GCMs, and CORDEX-RCMs for the period of 1951–2005. Observed mean annual number of rainy days varied between 20 and 200 days with higher values in the Northeast India and Western Ghats (Figure 6a). Among the BEST-GCMs, CMCC-CMS and MPI-ESM-MR underestimated number of rainy days, while CNRM-CM5 and GFDL-CM3 overestimated the number of rainy days in the majority of India (Figures 6e–6h). Among the HOST-GCMs, IPSL-CM5A-LR and MPI-ESM-LR underestimated the number of rainy days, while among the CORDEX-RCMs, COSMO-CLM model showed an underestimation in the majority of India except the northern and northeast parts of India (Figures 6i–6p), which can be attributed to a dry bias present in its host GCM (i.e., MPI-ESM-LR). While we do not notice any relationship between the models' ability to simulate the number of rainy days and the extreme precipitation indices, results indicate a similar bias in the number of rainy days in the CORDEX-RCMs and their HOST-GCMs. All-India bias in the number of rainy days varied between −24 and 43, −22 and 62, and −39 and 31 days in the BEST-GCMs, HOST-GCMs, and CORDEX-RCMs, respectively. Moreover, ensemble mean bias in the number of rainy days was 4.4, 7.4, and 5.0 days in the BEST-GCMs, HOST-GCMs, and CORDEX-RCMs, respectively. These results show that bias in the number of rainy days was improved (7.4 and 5.0 days) in the CORDEX-RCMs against their HOST-GCMs. Once again, we notice that intermodel variations in the bias in the number of rainy days in the CORDEX-RCMs is similar to that found in the BEST-GCMs and HOST-GCMs. Bias in the number of rainy days may be associated with the timing of the monsoon withdrawal as discussed in *Sperber et al.* [2012] as well as with temporal and spatial scales of precipitation as reported by *Gutowski et al.* [2003].

3.3. Trends in Annual Maximum Precipitation

We estimated changes in the observed and the model-simulated AMP during the period of 1951–2005 (Figure 7) using the nonparametric Mann-Kendall test. Observed trends in AMP showed a significant decline (30–40%) between 1951 and 2005 especially in northern India and in parts of the Gangetic Plain (Figure 7a). On the other hand, increasing trends in AMP were noticed in Jammu and Kashmir and parts of west central India. Overall there is a mixed nature of changes with a high spatial variability in AMP during the period of 1951–2005 as reported by *Ghosh et al.* [2012]. Most of the models, regardless of GCMs or RCMs, failed to capture the observed trends and associated spatial variability in AMP during the period of 1951–2005. GFDL-CM3, CNRM-CM5, and MPI-ESM-MR somewhat captured declining trends in AMP in the Gangetic Plain region; however, most of them failed to reproduce trends in northwestern India (Figures 7e–7h). On the other hand, the HOST-GCMs and CORDEX-RCMs (Table 2) largely failed to reproduce trends in AMP in the majority of India (Figures 7i–7p). All-India median trend in AMP varied between 0.83 and 6.2, 3.3 and 9.8, and 0.68 and 4.8% against the observed −6.0% in the BEST-GCMs, HOST-GCMs, and CORDEX-RCMs, respectively (Table 4). Ensemble mean trends in AMP in the BEST-GCMs, HOST-GCMs, and CORDEX-RCMs were 4.7, 7.5,

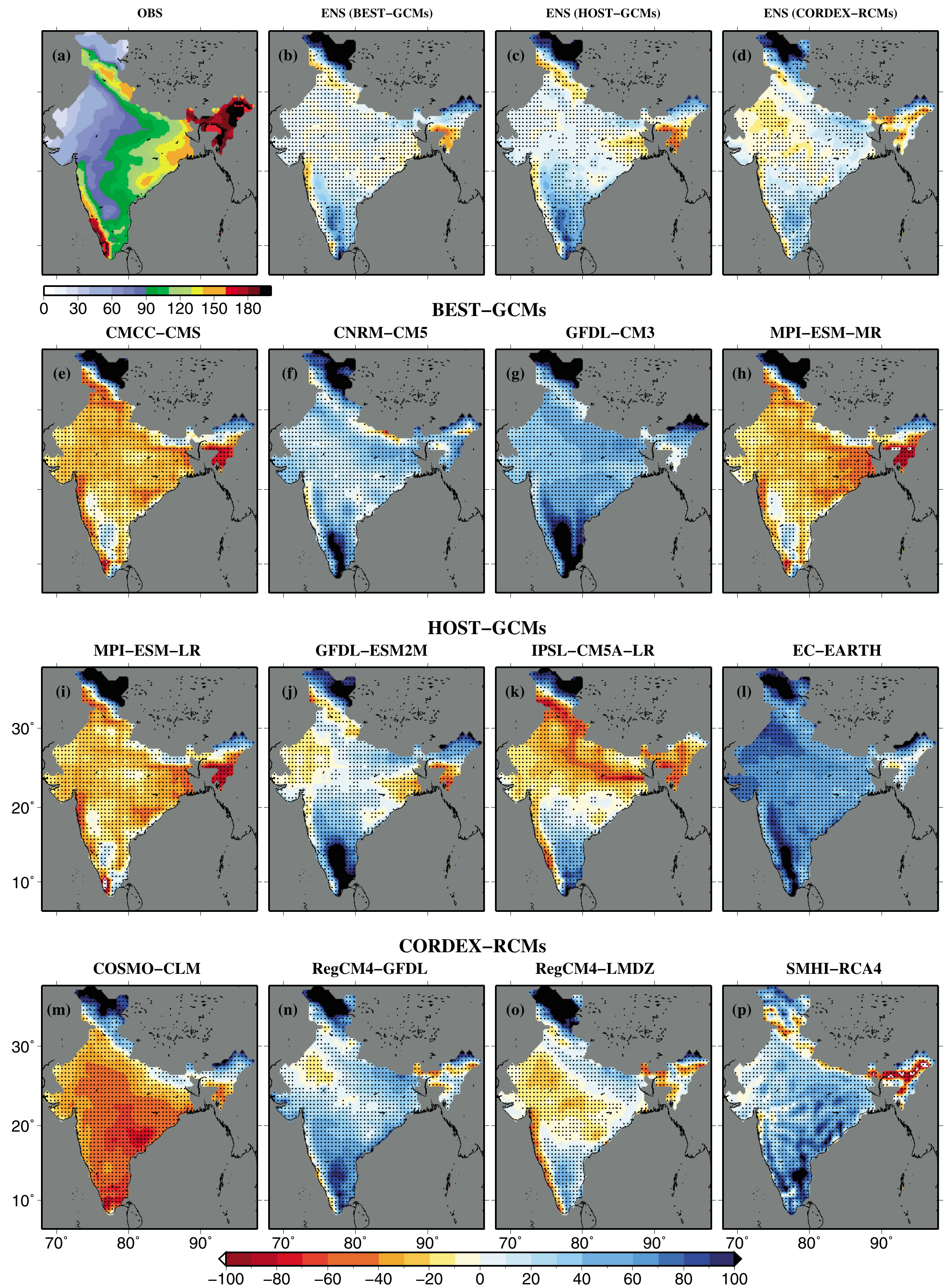

Figure 6. (a) Observed mean annual number of rainy days for the period of 1951–2005; (b–d) ensemble mean bias (days) in number of rainy days in the BEST-GCMs (CMCC-CMS, CNRM-CM5, GFDL-CM3, and MPI-ESM-MR), HOST-GCMs (MPI-ESM-LR, GFDL-ESM2M, IPSL-CM5A-LR, and EC-EARTH), and CORDEX-RCMs (COSMO-CLM, RegCM4-GFDL, RegCM4-LMDZ, and SMHI-RCA4); and (e–p) bias for the individual models in the BEST-GCMs, HOST-GCMs, and CORDEX-RCMs. Bias for the BEST-GCMs, HOST-GCMs, and CORDEX-RCMs was estimated for the period of 1951–2005. Stippling shows grid cells where mean is significantly different than observed mean as estimated by the rank sum test. Stippling in Figures 6b–6d shows grid cells where mean is significantly different than observed mean in all the models in the BEST-GCMs, HOST-GCM, and CORDEX-RCMs.

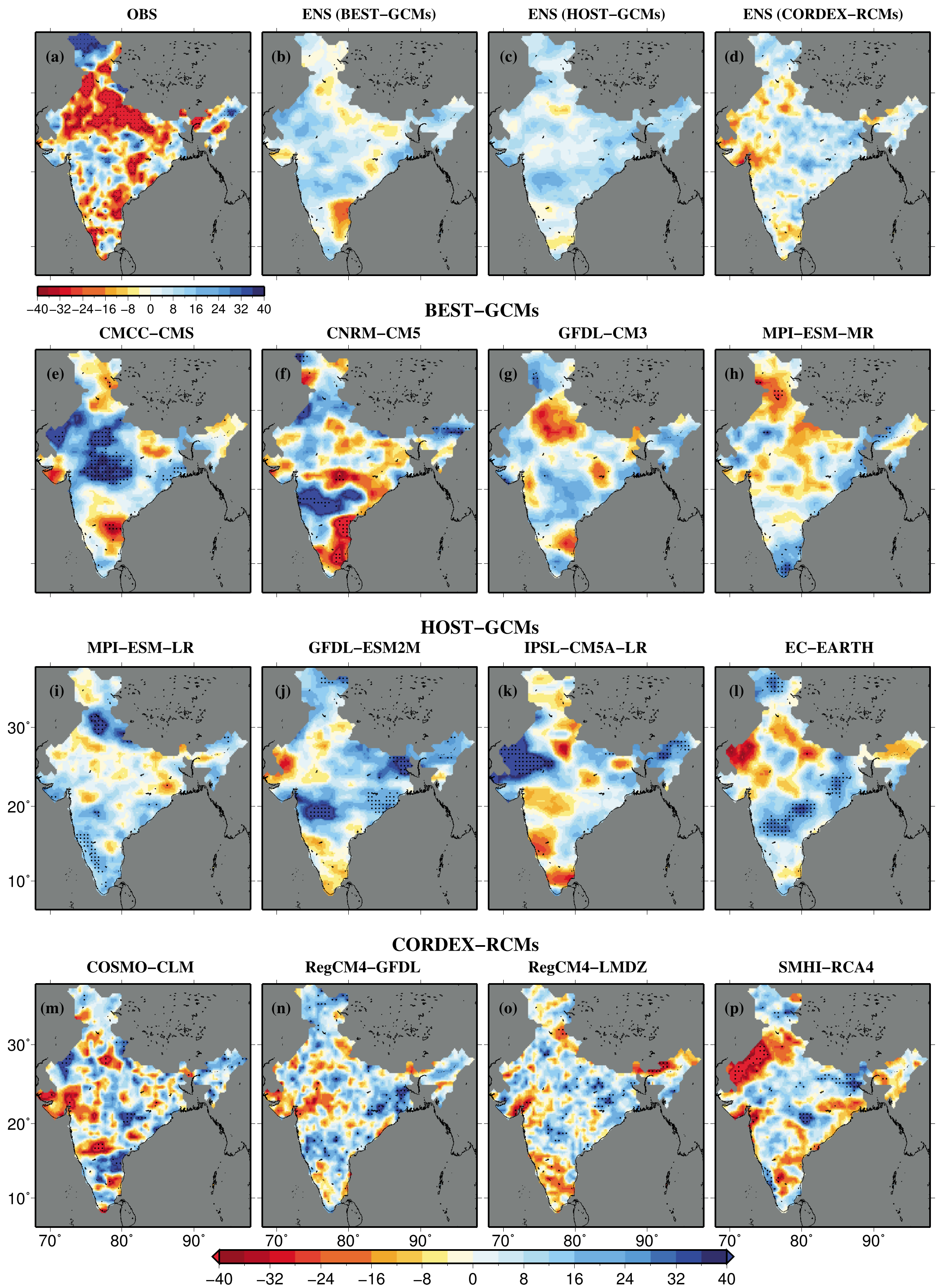

Figure 7. (a) Observed trend (%) in annual maximum precipitation (AMP) during the period of 1951–2005; (b–d) ensemble mean trend (%) in AMP in the BEST-GCMs, HOST-GCMs, and CORDEX-RCMs; and (e–p) trend (%) in AMP in the individual models. Trends for the BEST-GCMs, HOST-GCMs, and CORDEX-RCMs were estimated for the period of 1951–2005.

Table 4. All-India Median Bias in AMP, P-FREQ, PI-5, H-NH, 1 Day 25–100 Year Return Period, and Change in AMP (%) During 1951–2005 in the BEST-GCMs, HOST-GCMs, and CORDEX-RCMs

Index	BEST-GCMs				
	CMCC-CMS	CNRM-CM5	GFDL-CM3	MPI-ESM-MR	Ensemble
AMP (%)	−12.2	9.0	−16.1	−11.0	−6.56
P-FREQ (events/year)	−0.27	−0.04	−0.30	−0.23	−0.16
PI-5 (%)	−12.30	−13.00	−14.50	−9.00	−10.60
H-NH (%)	−0.07	−1.18	−1.08	−0.05	−0.53
1 day 25 year (%)	−16.60	22.32	−13.40	−20.00	−5.53
1 day 50 year (%)	−19.30	22.50	−15.10	−22.50	−7.00
1 day 100 year (%)	−22.20	23.50	−15.14	−26.00	−8.25
Trends in AMP (%)	6.28	2.97	5.78	0.83	4.79
			HOST-GCMs		
	EC-EARTH	GFDL-ESM2M	IPSL-CM5A-LR	MIP-ESM-LR	Ensemble
AMP (%)	−33.77	−14.07	−53.10	−16.85	−27.66
P-FREQ (events/year)	−0.71	−0.27	−0.82	−0.38	−0.49
PI-5 (%)	−26.16	−13.48	−50.26	−13.40	−24.58
H-NH (%)	−1.66	−1.60	−2.29	−0.39	−1.30
1 day 25 year (%)	−36.57	−3.52	−50.46	−26.00	−26.79
1 day 50 year (%)	−35.71	1.93	−48.41	−29.05	−26.42
1 day 100 year (%)	−34.52	7.30	−47.19	−32.39	−24.94
Trends in AMP (%)	4.99	9.88	3.30	4.46	7.05
			CORDEX-RCMs		
	COSMO-CLM	RegCM4-GFDL	RegCM4-LMDZ	SMHI-RCA4	Ensemble
AMP (%)	54.89	19.87	−9.49	−3.82	21.31
P-FREQ (events/year)	0.82	0.55	−0.29	−0.29	0.49
PI-5 (%)	24.16	15.37	−11.93	−4.97	10.64
H-NH (%)	−0.16	−0.49	−0.95	−0.62	−0.06
1 day 25 year (%)	89.54	21.95	−8.62	0.87	30.79
1 day 50 year (%)	99.26	22.35	−7.57	3.93	34.31
1 day 100 year (%)	108.97	22.06	−6.18	7.24	38.28
Trends in AMP (%)	4.06	4.80	2.88	0.68	2.83

and 2.8%, respectively. These results highlight deficiencies in the models to capture observed trends in AMP during the period of 1951–2005. Observed trends in extreme precipitation over India remain unclear as disparate findings were reported. For instance, *Goswami et al.* [2006] reported increasing trends in extreme precipitation during the monsoon season over central India using a coarse resolution rainfall data set. However, *Ghosh et al.* [2012] and *Vittal et al.* [2013] found more spatial variability but no significant increases in extreme precipitation in the monsoon season in India. We notice the clear declining trends in AMP during the period of 1951–2005 in northwestern India and Gangetic Plain. *Bollasina et al.* [2011] argued that anthropogenic aerosol emissions resulted in declines in the Indian summer monsoon rainfall, while *Goswami et al.* [2006] reported a linkage between sea surface temperature in the Indian Ocean and extreme precipitation in India. Therefore, a representation of aerosols in the models [*Laprise*, 2014] as well as trends in SST over the Indian Ocean can be associated with the deficiencies in simulation of the observed trends in the models. Furthermore, models often show a little skill for trends in precipitation as reported by *Kiktev et al.* [2003].

3.4. Bias in 1 Day Precipitation Maxima at 25–100 Year Return Period

Similar to 1 day precipitation maxima for 25 and 50 year return intervals (Figures S1 and S2 in the supporting information), we estimated 1 day 100 year precipitation maxima from the observed and the model-simulated precipitation. Observed 1 day 100 year precipitation maxima varied between 40 and 350 mm with similar spatial features as found for 1 day 25 and 50 year precipitation maxima (Figure 8). A majority of the CMIP5 models (except CNRM-CM5) in the BEST-GCMs underestimated 1 day 100 year precipitation maxima in the majority of India. Wet and dry biases were prominent in northern and central India, respectively (Figures 8e–8h). Most of the HOST-GCMs showed dry bias in 1 day 100 year precipitation maxima, which was dominant in the majority of India except in the parts of Jammu and Kashmir and peninsular India. The dry bias in IPSL-CM5A-LR was prominent in central India (Figure 8k). Consistent to 1 day 25 and 50 year precipitation maxima,

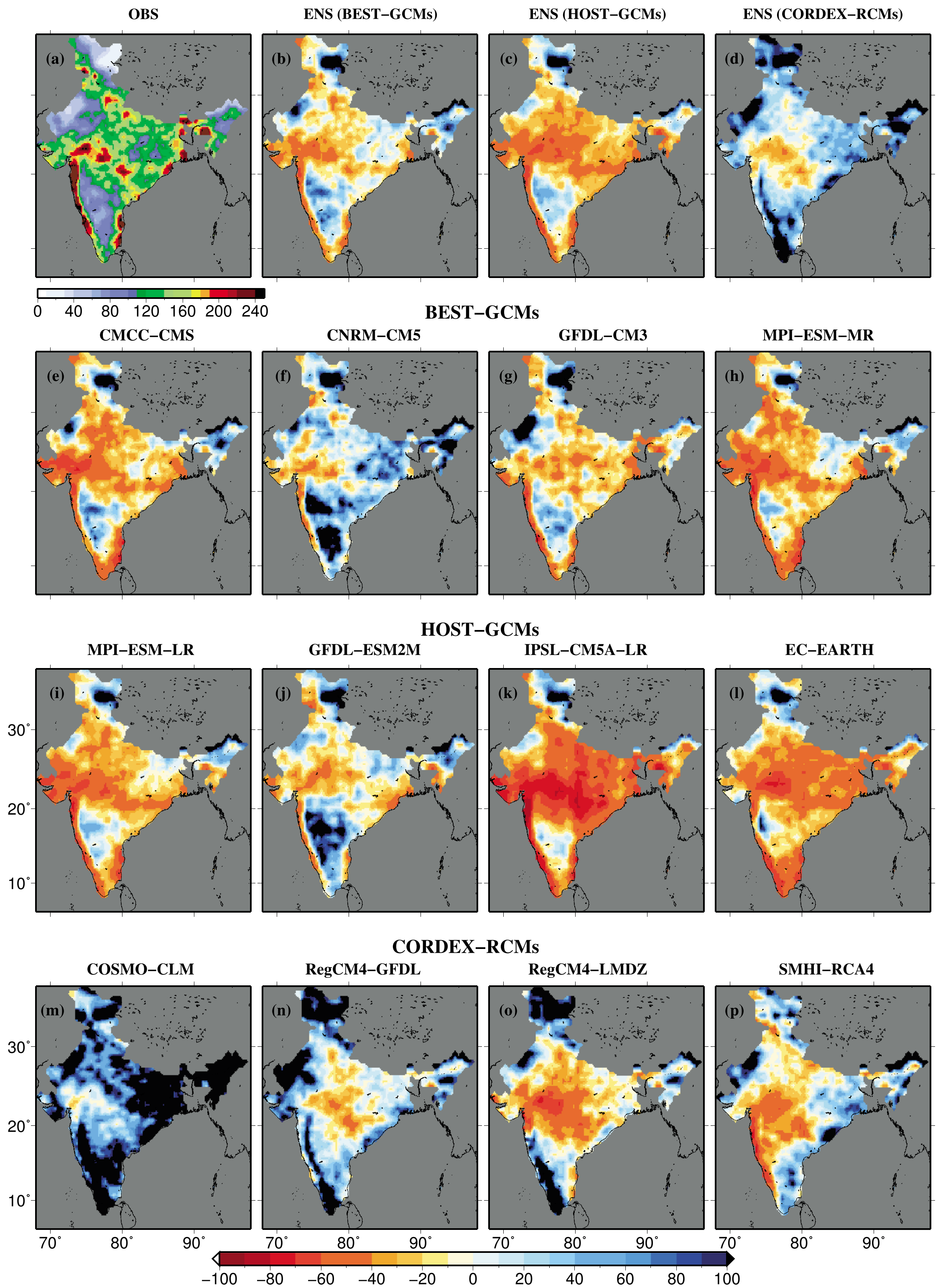

Figure 8. (a) Observed 1 day 100 year precipitation maxima for the period of 1951–2005; (b–d) ensemble mean bias (%) in 1 day 100 year precipitation maxima in the BEST-GCMs, HOST-GCMs, and CORDEX-RCMs; and (e–p) bias (%) in 1 day 100 year precipitation maxima in the individual models. Bias (%) for the BEST-GCMs, HOST-GCMs, and CORDEX-RCMs were estimated for the period of 1951–2005.

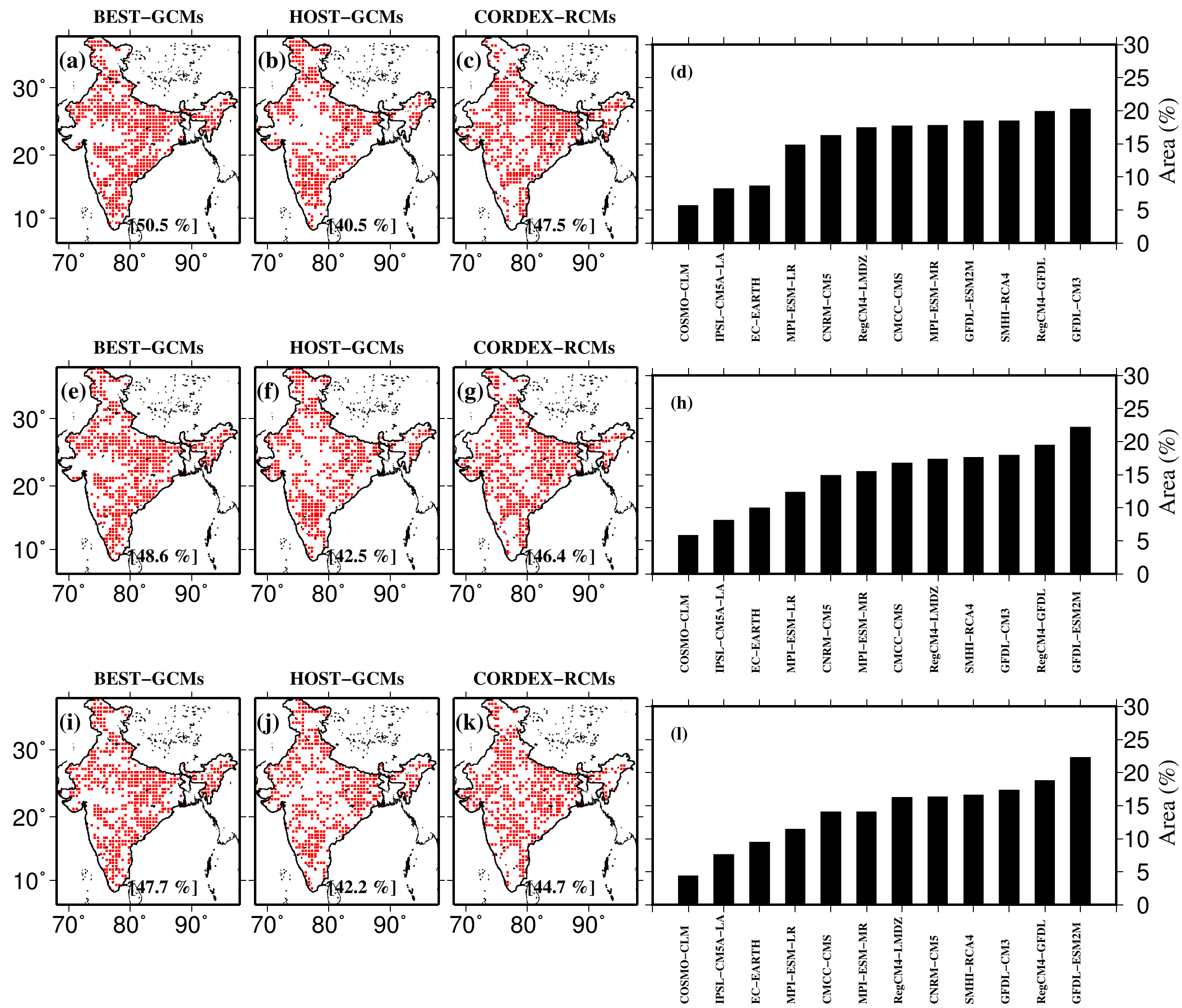

Figure 9. (a–c) Grid cells (in red) where models show appropriate bias (±10%) for hydrologic design purpose for 1 day precipitation maxima at 25 year return period and (d) models and the area (%) where bias is appropriate for design purpose for 1 day 25 year precipitation maxima. (e–g and i–k) Same as Figures 9a–9c but for 1 day precipitation maxima at 50 and 100 years. (h and l) Same as Figure 9d but for 50 and 100 years, respectively.

the CORDEX-RCMs showed both dry and wet bias that varied spatially and among models. For instance, the areas with dry bias were largely located in central India, while wet bias was more prominent in peninsular India (Figures 8m–8p). Among the CORDEX-RCMs, COSMO-CLM showed significant wet bias (more than 100%) across India (Figure 8m), while its HOST-GCM (MPI-ESM-LR) underestimated 1 day 100 year precipitation maxima. On the other hand, the bias in RegCM4-GFDL and its HOST-GCM (GFDL-ESM2M) was somewhat similar. These results highlight that the bias in the CORDEX-RCMs is not consistent with their HOST-GCMs. All-India ensemble mean median bias in the BEST-GCMs, HOST-GCMs, and CORDEX-RCMs was −8, −25, and 38%, respectively (Table 4). The two regional climate models that showed better performance to simulate 1 day 100 year precipitation maxima were RegCM4-LMDZ and SMHI-RCA4, while the other two (COSMO-CLM and RegCM4-GFDL) showed poorer performance than their HOST-GCMs (Table 4). We further notice that RegCM4-LMDZ and SMHI-RCA4 exhibited lower bias than any of the CMPI5 models in the BEST-GCMs. However, due to a large intermodal variability in bias in the CORDEX-RCMs, their ensemble mean performance was weaker than both the HOST-GCMs and the BEST-GCMs (Table 4). Changes in the nature of bias in the CORDEX-RCMs from their HOST-GCMs may be attributed to differences in parameterization, spatial resolution, and numerical schemes [*Rummukainen et al.*, 2001; *Fowler et al.*, 2007a, 2007b; *Tripathi and Dominguez*, 2013]. Increased resolution in the RCMs from the CMIP5 models might have led to a better representation of extreme precipitation intensities in RegCM4-LMDZ and SMHI-RCA4 as reported in *Gutowski et al.* [2003]; however, this was not consistent in all the

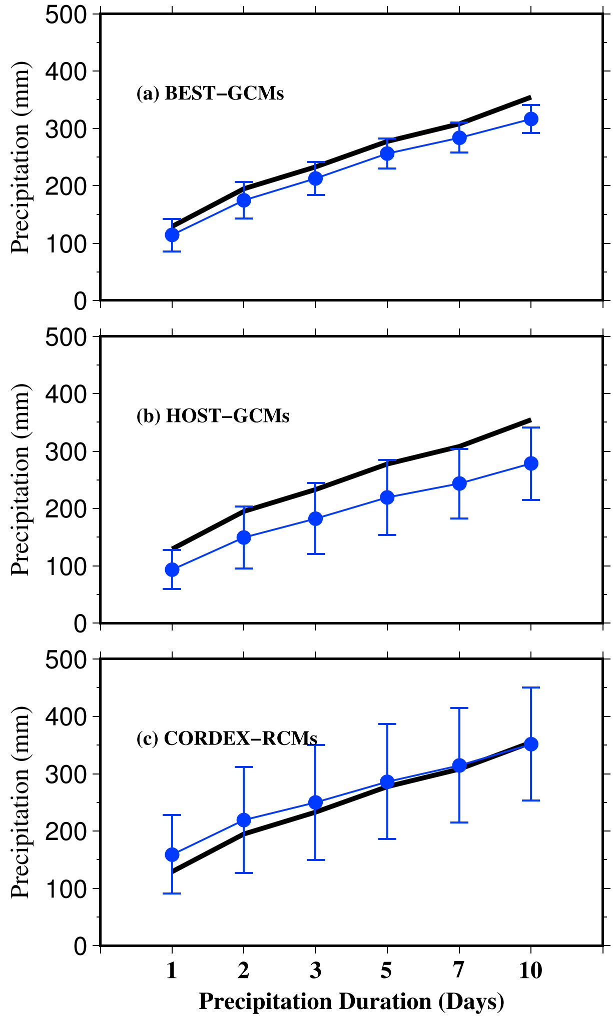

Figure 10. Observed (black) and model-simulated (blue) intensity-duration-frequency (IDF) curves for all-India averaged annual maximum precipitation for the period of 1951–2005. Error bars represent intermodel variation in (a) BEST-GCMs, (b) HOST-GCMs, and (c) CORDEX-RCMs. (Return period = 100 years.)

CORDEX-RCMs. *Tripathi and Dominguez* [2013] found that a fine-grid resolution resulted in overestimations in summer precipitation in Arizona, while 10 km resolution resulted in better simulations of precipitation extremes than that of 50 km. Similar findings were reported in *Rajendran et al.* [2013], who found that a 20 km resolution better captured the characteristics of the Indian summer monsoon and resolved fine-scale processes that contribute toward extreme precipitation.

Dry and wet biases as exhibited by the BEST-GCMs, HOST-GCMs, and CORDEX-RCMs can influence hydrologic and hydraulic designs. Underestimations in precipitation maxima by the models may increase risks of failures of hydrologic structures, while overestimations may lead to an increased cost of infrastructures. We considered ±10% bias in precipitation maxima appropriate for hydrologic and hydraulic designs as described in *Mishra et al.* [2012a, 2012b] and estimated the number of grid cells (or area in percentage) where the models show a reasonable performance (bias less than ± 10%) to simulate 1 day precipitation maxima at 25–100 year return intervals (Figure 9). Moreover, we estimated the combined area (in %) where any one of the selected models (among the BEST-GCMs, HOST-GCMs, and CORDEX-RCMs) can provide useful estimates of precipitation maxima for the design purposes. For 1 day 25 year precipitation maxima, the performance of the BEST-GCMs, HOST-GCMs, and CORDEX-RCMs was appropriate for the design purposes at 50.5, 40.5, and 47.5% grid cells in India, respectively (Figures 9a–9c). Other than GFDL-CM3 and RegCM4-GFDL, all the other models showed a reasonable performance in less than 20% of the area (Figure 9d). For 1 day 50 year precipitation maxima, the BEST-GCMs, HOST-GCMs, and CORDEX-RCMs showed an appropriate performance at 48.6, 42.5, and 46.4% of grid cells across India (Figures 9e–9g). Furthermore, only GFDL-ESM2M model exhibited a reasonable performance for the design purpose at more than 20% of the grid cells in India (Figure 9h). GFDL-ESM2M also showed the best performance for 1 day 100 year return intervals, while the bias was appropriate at 47.7, 42.2, and 44.7% grid cells from the BEST-GCMs, HOST-GCMs, and CORDEX-RCMs, respectively (Figures 9i–9l). We noticed that the BEST-GCMs showed a lower bias in the majority of central India, with a higher bias in western India. On the other hand, in the CORDEX-RCMs and their HOST-GCMs, a lower bias was more evenly distributed across India except the parts of Jammu and Kashmir. Moreover, we found a negligible area where all the models among the BEST-GCMs, HOST-GCMs, and CORDEX-RCMs consistently showed lower dry/wet biases which can be considered appropriate for the design purpose. These results highlight that despite the dynamical downscaling; the CORDEX-RCMs fail to cover more than 50% area where values can be used for the hydrologic and hydraulic designs. Moreover, the BEST-GCMs showed a better performance than the CORDEX-RCMs or their HOST-GCMs. We argue that despite the

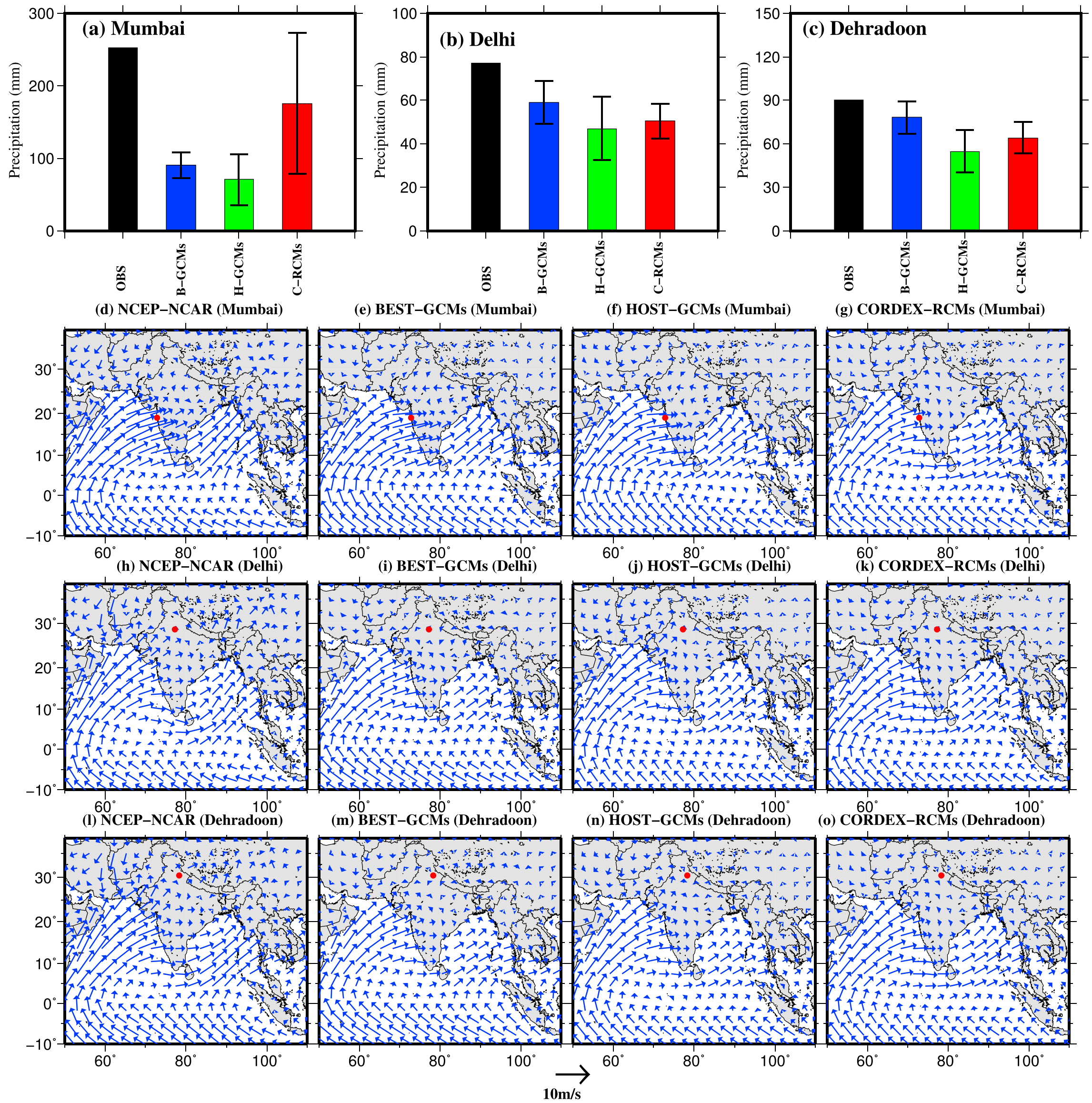

Figure 11. (a–c) Observed and ensemble mean precipitation for the top 20 extreme precipitation events during the period of 1951–2005 from the APHRODITE, BEST-GCMs, HOST-GCMs, and CORDEX-RCMs; (d–g) composite wind patterns for precipitation extremes in Mumbai from the NCEP-NCAR, BEST-GCMs, HOST-GCMs, and CORDEX-RCMs; (h–k) same as Figures 11d–11g but for Delhi; and (l–o) same as Figures 11d–11g but for Dehradun. Red dots represent location of the selected cities.

dynamical downscaling, the bias in the CORDEX-RCMs is similar to those found in their HOST-GCMs, which once again underscores the need for further improvements in the RCMs. A disagreement among the RCMs to simulate precipitation maxima in India remains high (at least similar to the CMIP5 GCMs) which may lead to a significant uncertainty in the projections of design maxima.

We constructed intensity-duration-frequency (IDF) curves using AMP for 1–10 day durations for the period of 1951–2005 (Figure 10). Precipitation maxima at 1–10 day durations and 100 year return period were estimated using the GEV distribution fitted through the L moment based approach. We estimated all-India median precipitation maxima at the selected durations from the individual models, and then ensemble mean was taken, which was compared with the observed precipitation maxima obtained from the APHRODITE data. We notice that the ensemble mean precipitation maxima from the BEST-GCMs underestimated the observed precipitation maxima at 1–10 day durations and at 100 year return period (Figure 10a). Underestimations in multiday precipitation maxima in the HOST-GCMs were higher than that obtained from

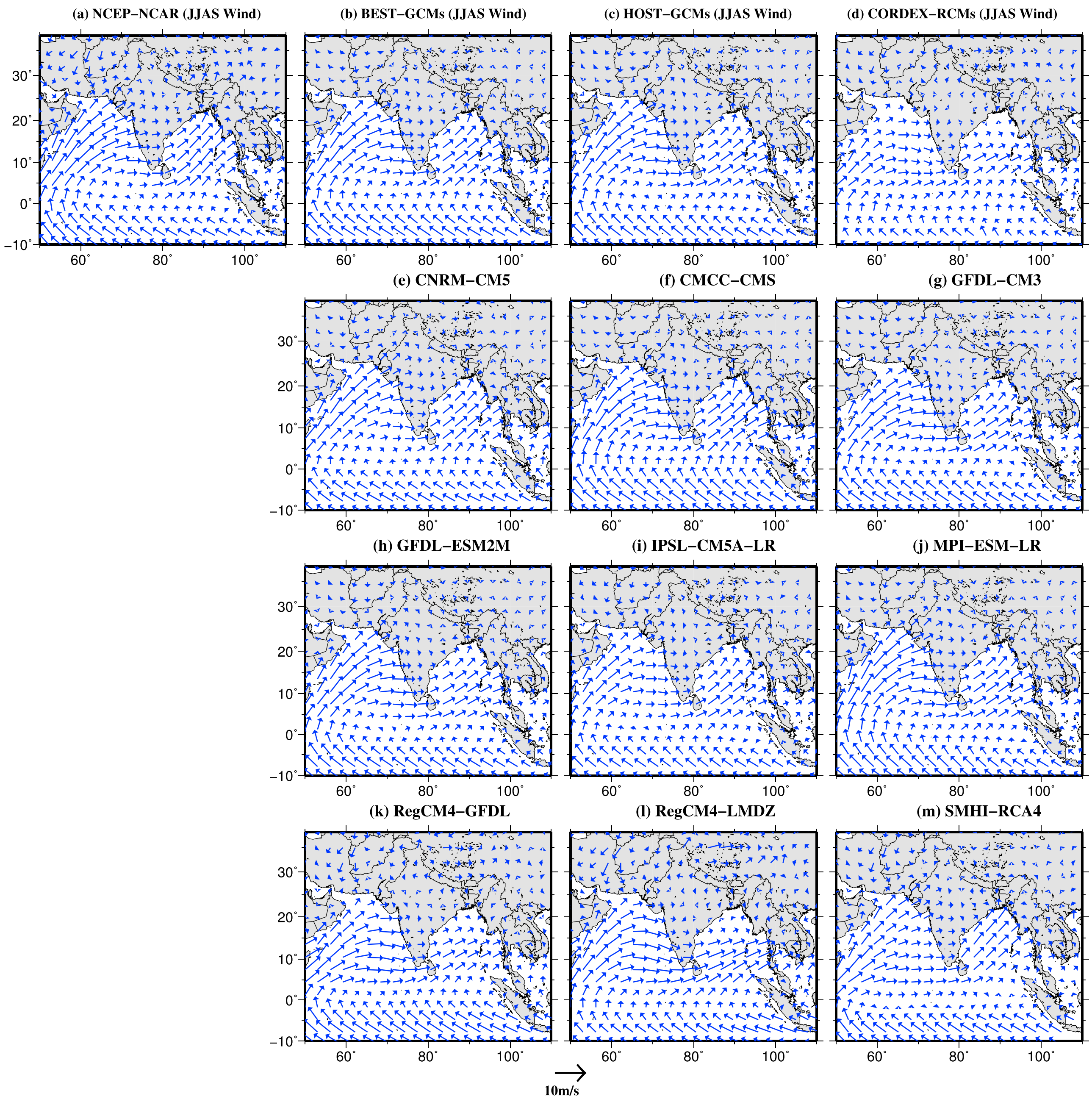

Figure 12. Climatological wind for the monsoon season (June to September) from (a) NCEP-NCAR for the period of 1951–2005; (b–d) ensemble mean climatological wind for BEST-GCMs, HOST-GCMs, and CORDEX-RCMs; and (e–m) climatological wind for the monsoon season from the individual models.

the BEST-GCMs (Figure 10b). The CORDEX-RCMs overestimated multiday precipitation maxima at 100 year return period for 1–7 day durations (Figure 10c). However, intermodel variations in multiday precipitation maxima in the CORDEX-RCMs were significantly higher than that found in the BEST-GCMs and HOST-GCMs (Figures 10a–10c). The high intermodel variations in the CORDEX-RCMs can be attributed to the presence of both dry and wet biases in AMP as shown in the results.

3.5. Precipitation Extremes and Large-Scale Wind Patterns

We estimated mean precipitation intensity for the top 20 events during the monsoon season (1951–2005) and their composite wind patterns for the three urban areas (Mumbai, Delhi, and Dehradun). We were interested to understand the association between extreme precipitation events and the large-scale wind patterns (Figure 11). Observed mean precipitation intensity for the top 20 events was 260 mm, which was underestimated by the BEST-GCMs, HOST-GCMs, and CORDEX-RCMs. The CORDEX-RCMs performed better than the BEST-GCMs as well as HOST-GCMs; however, those showed larger uncertainty (as shown by intermodel variations; Figure 11a). Among the CORDEX-RCMs, most of the models showed an improved performance for orographic precipitation in the Western Ghats except SMHI-RCA4, which showed a high dry bias in the region. Here one should note the larger uncertainty in the CORDEX-RCMs to simulate extreme precipitation over Mumbai despite a better performance than the GCMs which can be attributed to the presence of dry and wet biases in AMP. Mean extreme precipitation intensity over Delhi was better simulated by the BEST-GCMs with relatively lower intermodel variations (Figure 11b). The CORDEX-RCMs showed a large dry bias in precipitation extremes over Delhi; however, the bias was improved in comparison to their HOST-GCMs. Similar to Delhi, the BEST-GCMs exhibited a better performance to reproduce extreme precipitation intensity over Dehradun. Interestingly, the CORDEX-RCMs displayed an improved extreme precipitation intensity than that of their HOST-GCMs, which highlights an improvement in the ensemble mean performance (Figures 11a–11c).

We evaluated composite surface wind patterns from the RCMs and GCMs against the NCEP-NCAR reanalysis for all three selected cities (i.e., Mumbai, Delhi, and Dehradun). Ensemble mean composite wind patterns were constructed using the mean wind fields for the top 20 extreme precipitation events from the individual models. Composite wind patterns from the NCEP-NCAR reanalysis associated with extreme precipitation over Mumbai showed a strong westerly flow of high wind velocities in the Arabian Sea, which crossed the southern peninsula and moved into the Bay of Bengal (Figure 11d). This observed feature was well reproduced by the ensemble mean patterns from the BEST-GCMs, HOST-GCMs, and CORDEX-RCMs (Figures 11e–11g) but with disparities in wind velocities. We notice that despite weaker wind composites in the Arabian Sea and West Bengal (Figure 11g), the CORDEX-RCMs better simulated extreme precipitation intensity over Mumbai (Figure 11a), which can be attributed to large intermodel variations (two out of three models performed much better than SMHI-RCA4). Similar patterns for the surface winds were observed for extreme precipitation intensity over Delhi and Dehradun (Figures 11h and 11l) with stronger winds in northwestern India (toward Delhi and Dehradun). While the BEST-GCMs and HOST-GCMs captured large-scale patterns in a reasonable manner, the differences in surface wind velocity can be noticed in northwestern India. Moreover, we notice weaker winds in the CORDEX-RCMs associated with extreme precipitation events over Delhi and Dehradun (Figures 11k and 11o).

Figure 12 shows climatological wind field for the monsoon season (June-July-August-September (JJAS)) from the NCEP-NCAR and global and regional climate models. For GCMs and RCMs, we constructed ensemble mean climatological wind fields for the monsoon season during the period of 1951–2005, which were compared with wind fields from the NCEP-NCAR reanalysis data. Since most rainfall occurs during the monsoon season in India, differences in climatological wind fields in GCMs/RCMs from the reanalysis data can provide insights about their ability to simulate extreme precipitation. Ensemble mean climatological wind fields for the monsoon season from BEST-GCMs and HOST-GCMs resemble well the wind fields from the reanalysis data (Figures 12a–12c); however, disparities can be seen in ensemble mean wind field from the CORDEX-RCMs (Figure 12d). Climatological wind fields from the individual models reveal weaker monsoonal wind flow in IPSL-CM5A-LR model which could be associated with large dry bias for mean monsoon season precipitation as well as extremes [*Menon et al.*, 2013]. On the other hand, weaker wind fields in the Bay of Bengal in RegCM4-GFDL and RegCM4-LMDZ may be associated with their HOST-GCMs (Figure 12).

4. Conclusions

Our results, consistent with the findings of *Racherla et al.* [2012], showed that dynamical downscaling does not necessarily improve simulation of extreme precipitation events over India. Out of four RCMs in the CORDEX South Asia program, only two simulated the extreme precipitation indices better than their HOST-GCMs. In the other two models (COSMO-CLM and RegCM4-GFDL), the bias in extreme precipitation events was higher than that of their HOST-GCMs (Table 4). Furthermore, we notice that a negative bias present in the EC-EARTH and GFDL-ESM2M turned to a large positive bias after dynamical downscaling in COSMO-CLM and RegCM4-GFDL models. We find a significant improvement in bias after the dynamical downscaling in the two models (RegCM4-LMDZ and SMHI-RCA4). Therefore, model skills may not be directly linked solely with the resolution; rather it could be associated with location, parameterization, and boundary conditions [*Maurer and Hidalgo*, 2008]. In particular, a major challenge for many GCMs is to capture the observed distribution of mean summer monsoon precipitation over South Asia and its variability, which are closely tied to the large-scale monsoon dynamics and organization of convective systems [*Choudhury and Krishnan*, 2011; *Sabin et al.*, 2013]. This implies that the realism of dynamical downscaling of precipitation over the South Asian region is critically dependent on the physical parameterization schemes used in the model. The influence of model resolution on skills in precipitation simulations has been discussed in many studies [*Rojas*, 2006; *Tripathi and Dominguez*, 2013; *Walther et al.*, 2013]. However, spatial resolution is not the only factor that controls skills of extreme precipitation simulations; additional efforts are required to understand the potential role of spatial resolution on extreme precipitation over India.

We notice that for most of the selected extreme precipitation indices (Table 4), the BEST-GCMs showed better skills than the CORDEX-RCMs and their HOST-GCMs based on ensemble mean. For instance, the ensemble mean bias in annual maximum precipitation in the BEST-GCMs, HOST-GCMs, and CORDEX-RCMs was −6.5, 27.66, and 21.31%, respectively. Here, one may notice that the BEST-GCMs were selected after a careful evaluation of the 32 CMIP5 models against the observed precipitation extremes in India (Figure 1 and Table 3), while the sample size of the CORDEX-RCMs is far lower. We found that spatial interpolation of daily precipitation at a higher resolution may itself cause an uncertainty and differences in the skills as reported by *Chen and Knutson* [2008]. The major problem associated with the poor performance of the CORDEX-RCMs in comparison to the BEST-GCMs can be attributed to intermodel variations. *Giorgi and Francisco* [2000] reported that the largest source of uncertainty in regional climate models is associated with intermodel variability. High intermodel variations in the CORDEX-RCMs leads to a large bias in their ensemble mean; on the other hand, relatively low intermodel variations in the BEST-GCMs results in a better performance. The large intermodel variations present in the CORDEX-RCMs highlight the need of more regional climate models with a large number of boundary conditions as suggested by *Fowler and Ekström* [2009]. Moreover, future work may be dedicated to select boundary conditions which have a lower bias (possibly the BEST-GCMs) for downscaling experiments. Simulation of the atmospheric variables by GCMs not just at the surface level but also in the upper troposphere will make the model evaluation process more effective.

Climate projections for hydrologic application are required at a high resolution with a lower uncertainty [*Wood et al.*, 2004; *Fowler et al.*, 2007a, 2007b]. Our results showed that ensemble mean of the BEST-GCMs outperformed the CORDEX-RCMs to simulate precipitation maxima at 1–10 day durations (Table 4). For instance, ensemble mean bias in the CORDEX-RCMs was significantly higher than that of the BEST-GCMs. While the CORDEX-RCMs can better resolve orographic precipitation in complex topographic regions (e.g., Western Ghats and foothills of the Himalaya), a large bias in simulation of precipitation maxima limits their usefulness for the hydrologic and hydraulic designs. The large intermodel variations present in the CORDEX-RCMs may also play a major role in their use for hydrologic applications. From the results, it appears that the BEST-GCMs may be better suitable for a decision making related to hydrology because of the lower bias and uncertainty. Regional climate models may be valuable; however, significant improvements in the model parameterization, spatial resolution, and boundary conditions are required to reduce bias and uncertainty (intermodel variability). Outputs from regional climate models may be bias corrected further to use them for the hydrologic impact studies [*Wood et al.*, 2004; *Christensen et al.*, 2008; *Piani et al.*, 2010; *Teutschbein and Seibert*, 2012].

Acknowledgments
The first author acknowledges funding from the Varahamihir Ministry of Earth Science Fellowship of India. The research was partially funded by the United States National Science Foundation (NSF) Expeditions in Computing grant 1029711. Data used in this study can be obtained from APHRODITE (http://www.chikyu.ac.jp/precip/) and CORDEX South Asia (http://cccr.tropmet.res.in/cordex/files/downloads.jsp). The CMIP5 models data can be obtained from the Program for Climate Model Diagnosis and Intercomparison (PCMDI) archive of the U.S. Department of Energy at Lawrence Livermore National Laboratory (LLNL). We acknowledge Bodo Ahrens and Shakeel Asharaf from Goethe-Universitaet Frankfurt for providing outputs of COSMO-CLM and Nikulin Grigory and Colin Jones, Rossby Centre, Sweden, for providing outputs of SMHI-RCA4.

References

Allan, R. P., C. Liu, M. Zahn, D. A. Lavers, E. Koukouvagias, and A. Bodas-Salcedo (2014), Physically consistent responses of the global atmospheric hydrological cycle in models and observations, *Surv. Geophys.*, *35*(3), 533–552, doi:10.1007/s10712-012-9213-z.

Bollasina, M. A., Y. Ming, and V. Ramaswamy (2011), Anthropogenic aerosols and the weakening of the South Asian summer monsoon, *Science*, *334*(6055), 502–505.

Chaturvedi, R. K., J. Joshi, M. Jayaraman, G. Bala, and N. H. Ravindranath (2012), Multi-model climate change projections for India under representative concentration pathways, *Curr. Sci.*, *103*(7), 791–802.

Chen, C.-T., and T. Knutson (2008), On the verification and comparison of extreme rainfall indices from climate models, *J. Clim.*, *21*(7), 1605–1621.

Choudhury, A. D., and R. Krishnan (2011), Dynamical response of the South Asian monsoon trough to latent heating from stratiform and convective precipitation, *J. Atmos. Sci.*, *68*, 1347–1363.

Christensen, J. H., and O. B. Christensen (2003), Climate modelling: Severe summertime flooding in Europe, *Nature*, *421*(6925), 805–806.

Christensen, J. H., F. Boberg, O. B. Christensen, and P. Lucas-Picher (2008), On the need for bias correction of regional climate change projections of temperature and precipitation, *Geophys. Res. Lett.*, *35*, L20709, doi:10.1029/2008GL035694.

Coumou, D., and S. Rahmstorf (2012), A decade of weather extremes, *Nat. Clim. Change*, *2*(7), 491–496.
Déqué, M., D. P. Rowell, D. Lüthi, F. Giorgi, J. H. Christensen, B. Rockel, D. Jacob, E. Kjellström, M. De Castro, and B. van den Hurk (2007), An intercomparison of regional climate simulations for Europe: Assessing uncertainties in model projections, *Clim. Change*, *81*(1), 53–70.
Fowler, H. J., and M. Ekström (2009), Multi-model ensemble estimates of climate change impacts on UK seasonal precipitation extremes, *Int. J. Climatol.*, *29*(3), 385–416.
Fowler, H. J., and R. L. Wilby (2010), Detecting changes in seasonal precipitation extremes using regional climate model projections: Implications for managing fluvial flood risk, *Water Resour. Res.*, *46*, W03525, doi:10.1029/2008WR007636.
Fowler, H. J., M. Ekström, S. Blenkinsop, and A. P. Smith (2007a), Estimating change in extreme European precipitation using a multimodel ensemble, *J. Geophys. Res.*, *112*, D18104, doi:10.1029/2007JD008619.
Fowler, H. J., S. Blenkinsop, and C. Tebaldi (2007b), Linking climate change modelling to impacts studies: Recent advances in downscaling techniques for hydrological modelling, *Int. J. Climatol.*, *27*(12), 1547–1578, doi:10.1002/joc.1556.
Ghosh, S., D. Das, S.-C. Kao, and A. R. Ganguly (2012), Lack of uniform trends but increasing spatial variability in observed Indian rainfall extremes, *Nat. Clim. Change*, *2*(2), 86–91.
Giorgi, F., and R. Francisco (2000), Evaluating uncertainties in the prediction of regional climate change, *Geophys. Res. Lett.*, *27*(9), 1295–1298, doi:10.1029/1999GL011016.
Goswami, B. N., V. Venugopal, D. Sengupta, M. S. Madhusoodanan, and P. K. Xavier (2006), Increasing trend of extreme rain events over India in a warming environment, *Science*, *314*(5804), 1442–1445.
Groisman, P. Y., T. R. Karl, D. R. Easterling, R. W. Knight, P. F. Jamason, K. J. Hennessy, R. Suppiah, C. M. Page, J. Wibig, and K. Fortuniak (1999), Changes in the probability of heavy precipitation: Important indicators of climatic change, *Clim. Change*, *42*(1), 243–283.
Guhathakurta, P., O. P. Sreejith, and P. A. Menon (2011), Impact of climate change on extreme rainfall events and flood risk in India, *J. Earth Syst. Sci.*, *120*(3), 359–373.
Gutowski, W. J., Jr., S. G. Decker, R. A. Donavon, Z. Pan, R. W. Arritt, and E. S. Takle (2003), Temporal-spatial scales of observed and simulated precipitation in central US climate, *J. Clim.*, *16*(22), 3841–3847.
Gutowski, W. J., Jr., R. W. Arritt, S. Kawazoe, D. M. Flory, E. S. Takle, S. Biner, D. Caya, R. G. Jones, R. Laprise, and L. R. Leung (2010), Regional extreme monthly precipitation simulated by NARCCAP RCMs, *J. Hydrometeorol.*, *11*(6), 1373–1379.
Harding, K. J., P. K. Snyder, and S. Liess (2013), Use of dynamical downscaling to improve the simulation of Central U.S. warm season precipitation in CMIP5 models, *J. Geophys. Res. Atmos.*, *118*, 12,522–12,536, doi:10.1002/2013JD019994.
Hosking, J. R. M., and J. R. Wallis (2005), *Regional Frequency Analysis: An Approach Based on L-Moments*, Cambridge Univ. Press, Cambridge.
Kalnay, E., M. Kanamitsu, R. Kistler, W. Collins, D. Deaven, L. Gandin, M. Iredell, S. Saha, G. White, and J. Woollen (1996), The NCEP/NCAR 40-year reanalysis project, *Bull. Am. Meteorol. Soc.*, *77*(3), 437–471.
Kao, S.-C., and A. R. Ganguly (2011), Intensity, duration, and frequency of precipitation extremes under 21st-century warming scenarios, *J. Geophys. Res.*, *116*, D16119, doi:10.1029/2010JD015529.
Kawazoe, S., and W. Gutowski (2013), Regional, very heavy daily precipitation in CMIP5 simulations, *J. Hydrometeorol.*, *14*, 1228–1242, doi:10.1175/JHM-D-12-0112.1.
Kharin, V. V., and F. W. Zwiers (2000), Changes in the extremes in an ensemble of transient climate simulations with a coupled atmosphere–ocean GCM, *J. Clim.*, *13*(21), 3760–3788.
Kharin, V. V., F. W. Zwiers, X. Zhang, and G. C. Hegerl (2007), Changes in temperature and precipitation extremes in the IPCC ensemble of global coupled model simulations, *J. Clim.*, *20*(8), 1419–1444.
Kiktev, D., D. M. Sexton, L. Alexander, and C. K. Folland (2003), Comparison of modeled and observed trends in indices of daily climate extremes, *J. Clim.*, *16*(22), 3560–3571.
Kishtawal, C. M., D. Niyogi, M. Tewari, R. A. Pielke, and J. M. Shepherd (2010), Urbanization signature in the observed heavy rainfall climatology over India, *Int. J. Clim.*, *30*(13), 1908–1916.
Krishnamurthy, C. K. B., U. Lall, and H.-H. Kwon (2009), Changing frequency and intensity of rainfall extremes over India from 1951 to 2003, *J. Clim.*, *22*(18), 4737–4746.
Laprise, R. (2014), Comment on "The added value to global model projections of climate change by dynamical downscaling: A case study over the continental U.S. using the GISS-ModelE2 and WRF models" by Racherla et al., *J. Geophys. Res. Atmos.*, *119*, 3877–3881, doi:10.1002/2013JD019945.
Leung, L. R., S. Zhong, Y. Qian, and Y. Liu (2004), Evaluation of regional climate simulations of the 1998 and 1999 East Asian Summer Monsoon using the GAME/HUBEX observational data, *J. Meteorol. Soc. Jpn.*, *82*(6), 1695–1713.
Mani, N. J., E. Suhas, and B. N. Goswami (2009), Can global warming make Indian monsoon weather less predictable?, *Geophys. Res. Lett.*, *36*, L08811, doi:10.1029/2009GL037989.
Mann, H. B. (1945), Nonparametric tests against trend, *Econometrica*, *13*, 245–259.
Maurer, E. P., and H. G. Hidalgo (2008), Utility of daily vs. monthly large-scale climate data: An intercomparison of two statistical downscaling methods, *Hydrol. Earth Syst. Sci.*, *12*(2), 551–563.
Menon, A., A. Levermann, J. Schewe, J. Lehmann, and K. Frieler (2013), Consistent increase in Indian monsoon rainfall and its variability across CMIP-5 models, *Earth Syst. Dyn.*, *4*(2), 1–24.
Min, S.-K., X. Zhang, F. W. Zwiers, and G. C. Hegerl (2011), Human contribution to more-intense precipitation extremes, *Nature*, *470*(7334), 378–381.
Mishra, V., and D. P. Lettenmaier (2011), Climatic trends in major U.S. urban areas, 1950–2009, *Geophys. Res. Lett.*, *38*, L16401, doi:10.1029/2011GL048255.
Mishra, V., K. A. Cherkauer, and S. Shukla (2010), Assessment of drought due to historic climate variability and projected future climate change in the midwestern United States, *J. Hydrometeorol.*, *11*, 46–68, doi:10.1175/2009JHM1156.1.
Mishra, V., F. Dominguez, and D. P. Lettenmaier (2012a), Urban precipitation extremes: How reliable are regional climate models?, *Geophys. Res. Lett.*, *39*, L03407, doi:10.1029/2011GL050658.
Mishra, V., J. M. Wallace, and D. P. Lettenmaier (2012b), Relationship between hourly extreme precipitation and local air temperature in the United States, *Geophys. Res. Lett.*, *39*, L16403, doi:10.1029/2012GL052790.
Mohapatra, P. K., and R. D. Singh (2003), Flood management in India, *Nat. Hazards*, *28*(1), 131–143.
O'Gorman, P. A., and T. Schneider (2009), The physical basis for increases in precipitation extremes in simulations of 21st-century climate change, *Proc. Natl. Acad. Sci. U.S.A.*, *106*(35), 14,773–14,777.
Piani, C., J. O. Haerter, and E. Coppola (2010), Statistical bias correction for daily precipitation in regional climate models over Europe, *Theor. Appl. Climatol.*, *99*(1–2), 187–192.
Racherla, P. N., D. T. Shindell, and G. S. Faluvegi (2012), The added value to global model projections of climate change by dynamical downscaling: A case study over the continental U.S. using the GISS-ModelE2 and WRF models, *J. Geophys. Res.*, *117*, D20118, doi:10.1029/2012JD018091.

Rajeevan, M., J. Bhate, and A. K. Jaswal (2008), Analysis of variability and trends of extreme rainfall events over India using 104 years of gridded daily rainfall data, *Geophys. Res. Lett.*, *35*, L18707, doi:10.1029/2008GL035143.

Rajendran, K., S. Sajani, C. B. Jayasankar, and A. Kitoh (2013), How dependent is climate change projection of Indian summer monsoon rainfall and extreme events on model resolution?, *Curr. Sci.* (00113891), *104*(10), 1409.

Rojas, M. (2006), Multiply nested regional climate simulation for southern South America: Sensitivity to model resolution, *Mon. Weather Rev.*, *134*(8), 2208–2223.

Rosenberg, E. A., P. W. Keys, D. B. Booth, D. Hartley, J. Burkey, A. C. Steinemann, and D. P. Lettenmaier (2010), Precipitation extremes and the impacts of climate change on stormwater infrastructure in Washington State, *Clim. Change*, *102*(1–2), 319–349.

Rummukainen, M., J. Räisänen, B. Bringfelt, A. Ullerstig, A. Omstedt, U. Willén, U. Hansson, and C. Jones (2001), A regional climate model for northern Europe: Model description and results from the downscaling of two GCM control simulations, *Clim. Dyn.*, *17*(5–6), 339–359.

Sabin, T. P., R. Krishnan, J. Ghattas, S. Denvil, J.-L. Dufresne, F. Hourdin, and T. Pascal (2013), High resolution simulation of the South Asian monsoon using a variable resolution global climate model, *Clim. Dyn.*, doi:10.1007/s00382-012-1658-8.

Salathe, E. P., Jr., L. R. Leung, Y. Qian, and Y. Zhang (2010), Regional climate model projections for the state of Washington, *Clim. Change*, *102*(1–2), 51–75.

Sen, P. K. (1968), Estimates of the regression coefficient based on Kendall's tau, *J. Am. Stat. Assoc.*, *63*(324), 1379–1389.

Sillmann, J., V. V. Kharin, F. W. Zwiers, X. Zhang, and D. Bronaugh (2013), Climate extremes indices in the CMIP5 multimodel ensemble: Part 2. Future climate projections, *J. Geophys. Res. Atmos.*, *118*, 2473–2493, doi:10.1002/jgrd.50188.

Sperber, K. R., H. Annamalai, I.-S. Kang, A. Kitoh, A. Moise, A. Turner, B. Wang, and T. Zhou (2012), The Asian summer monsoon: An intercomparison of CMIP5 vs. CMIP3 simulations of the late 20th century, *Clim. Dyn.*, *41*(9–10), 2711–2744.

Sugiyama, M., H. Shiogama, and S. Emori (2010), Precipitation extreme changes exceeding moisture content increases in MIROC and IPCC climate models, *Proc. Natl. Acad. Sci. U.S.A.*, *107*(2), 571–575.

Sun, Y., S. Solomon, A. Dai, and R. W. Portmann (2007), How often will it rain?, *J. Clim.*, *20*(19), 4801–4818.

Taylor, K. E., R. J. Stouffer, and G. A. Meehl (2012), An overview of CMIP5 and the experiment design, *Bull. Am. Meteorol. Soc.*, *93*(4), 485–498.

Teutschbein, C., and J. Seibert (2012), Bias correction of regional climate model simulations for hydrological climate-change impact studies: Review and evaluation of different methods, *J. Hydrol.*, *456*, 12–29.

Toreti, A., P. Naveau, M. Zampieri, A. Schindler, E. Scoccimarro, E. Xoplaki, H. A. Dijkstra, S. Gualdi, and J. Luterbacher (2013), Projections of global changes in precipitation extremes from Coupled Model Intercomparison Project Phase 5 models, *Geophys. Res. Lett.*, *40*, 4887–4892, doi:10.1002/grl.50940.

Tripathi, O. P., and F. Dominguez (2013), Effects of spatial resolution in the simulation of daily and subdaily precipitation in the southwestern US, *J. Geophys. Res. Atmos.*, *118*, 7591–7605, doi:10.1002/jgrd.50590.

Vittal, H., S. Karmakar, and S. Ghosh (2013), Diametric changes in trends and patterns of extreme rainfall over India from pre-1950 to post-1950, *Geophys. Res. Lett.*, *40*, 3253–3258, doi:10.1002/grl.50631.

Walther, A., J.-H. Jeong, G. Nikulin, C. Jones, and D. Chen (2013), Evaluation of the warm season diurnal cycle of precipitation over Sweden simulated by the Rossby Centre regional climate model RCA3, *Atmos. Res.*, *119*, 131–139.

Watanabe, M., T. Suzuki, R. O'ishi, Y. Komuro, S. Watanabe, S. Emori, T. Takemura, M. Chikira, T. Ogura, and M. Sekiguchi (2010), Improved climate simulation by MIROC5: Mean states, variability, and climate sensitivity, *J. Clim.*, *23*(23), 6312–6335.

Wehner, M. F., R. L. Smith, G. Bala, and P. Duffy (2010), The effect of horizontal resolution on simulation of very extreme US precipitation events in a global atmosphere model, *Clim. Dyn.*, *34*(2–3), 241–247.

Wood, A. W., L. R. Leung, V. Sridhar, and D. P. Lettenmaier (2004), Hydrologic implications of dynamical and statistical approaches to downscaling climate model outputs, *Clim. Change*, *62*(1–3), 189–216.

Yatagai, A., K. Kamiguchi, O. Arakawa, A. Hamada, N. Yasutomi, and A. Kitoh (2012), APHRODITE: Constructing a long-term daily gridded precipitation dataset for Asia based on a dense network of rain gauges, *Bull. Am. Meteorol. Soc.*, *93*(9), 1401–1415.

Yue, S., and C. Y. Wang (2002), Regional Streamflow trend detection with consideration of both temporal and spatial correlation, *Int. J. Climatol.*, *22*, 933–946, doi:10.1002/joc.781.